Available online at www.sciencedirect.com
SCIENCE DIRECT®
Journal of Theoretical Biology 228 (2004) 195–215
Journal of Theoretical Biology
www.elsevier.com/locate/jtbi

Mathematical model of NF-κB regulatory module

Tomasz Lipniacki[a,b,c,*], Pawel Paszek[b], Allan R. Brasier[d], Bruce Luxon[c], Marek Kimmel[b,e]

[a] Institute of Fundamental Technological Research, Swietokrzyska 21, 00-049 Warsaw, Poland
[b] Department of Statistics, Rice University, 6100 Main Street MS-138, Houston, TX 77005, USA
[c] Division of Bioinformatics, University of Texas Medical Branch, Galveston, TX 77555-1060, USA
[d] Department of Internal Medicine, University of Texas Medical Branch, Galveston, TX 77555-1060, USA
[e] Institute of Automation, Silesian Technical University, 44-100 Geiwice, Poland

Received 2 September 2003; received in revised form 11 December 2003; accepted 23 December 2003

Abstract

The two-feedback-loop regulatory module of nuclear factor κB (NF-κB) signaling pathway is modeled by means of ordinary differential equations. The constructed model involves two-compartment kinetics of the activators IκB (IKK) and NF-κB, the inhibitors A20 and IκBα, and their complexes. In resting cells, the unphosphorylated IκBα binds to NF-κB and sequesters it in an inactive form in the cytoplasm. In response to extracellular signals such as tumor necrosis factor or interleukin-1, IKK is transformed from its neutral form (IKKn) into its active form (IKKa), a form capable of phosphorylating IκBα, leading to IκBα degradation. Degradation of IκBα releases the main activator NF-κB, which then enters the nucleus and triggers transcription of the inhibitors and numerous other genes. The newly synthesized IκBα leads NF-κB out of the nucleus and sequesters it in the cytoplasm, while A20 inhibits IKK converting IKKa into the inactive form (IKKi), a form different from IKKn, no longer capable of phosphorylating IκBα. After parameter fitting, the proposed model is able to properly reproduce time behavior of all variables for which the data are available: NF-κB, cytoplasmic IκBα, A20 and IκBα mRNA transcripts, IKK and IKK catalytic activity in both wild-type and A20-deficient cells. The model allows detailed analysis of kinetics of the involved proteins and their complexes and gives the predictions of the possible responses of whole kinetics to the change in the level of a given activator or inhibitor.

Keywords: Signaling pathways; Ordinary differential equations; NF-κB; A20; IκBα

1. Introduction

Nuclear factor κB (NF-κB) regulates numerous genes important for pathogen or cytokine inflammation, immune response, cell proliferation and survival. In mammals, the NF-κB family of transcription factors contains five members termed NF-κB1 (p50/p105), NF-κB2 (p52/p100), RelA(p65), RelB and cRel (reviewed in Tian and Brasier, 2003; Caamano and Hunter, 2002; Ghosh et al., 1998). NF-κB1 and NF-κB2 are synthesized as a 105 and 100 kDa precursors that must be post-translationally processed into the DNA binding subunits termed p50 and p52. The NF-κB members dimerize to form homo- and heteromeric complexes of various transcriptional activities. While RelA (p65), RelB and cRel carry the transcriptional activation domains, NF-κB1 (p50) and NF-κB2 (p52) lack transcriptional activity. In fact both p50 and p52 homodimers are repressive (Ghosh et al., 1998 and references therein). The ubiquitously expressed NF-κB1 (p50) and RelA(p65), heterodimer constitutes the most common inducible NF-κB binding activity. In contrast, NF-κB2, RelB and cRel are expressed specifically in lymphoid cells and tissues whereby play specific role in the immune response (Caamano and Hunter, 2002).

In resting cells, p50–65 heterodimers (referred herein as NF-κB) are sequestered in the cytoplasm by association with members of another family of proteins called IκB. This family of proteins includes IκBα, IκBβ, IκBε, IκBγ and Bcl-3, but also p105 and p100, which due to their C-terminal ankyrin-repeat regions have homologous functions to IκB. Most of the IκB-family inhibitory potential is carried by IκBα, whose synthesis is controlled by a highly NF-κB-responsive promoter

*Corresponding author. Department of Statistics, Rice University, 6100 Main Street MS-138, Houston, TX 77005, USA.
E-mail address: tomek@rice.edu, tlipnia@ippt.gov.pl (T. Lipniacki).

0022-5193/$ - see front matter © 2004 Elsevier Ltd. All rights reserved.
doi:10.1016/j.jtbi.2004.01.001

generating autoregulation of NF-κB signaling (Sun et al., 1993). Activation of NF-κB requires degradation of IκBα, which exposes the NF-κB nuclear localization sequence and allows NF-κB to translocate to the nucleus, bind to κB motifs present in the promoters of numerous genes and regulate their transcription. NF-κB specifically recognizes DNA elements with a consensus to sequence of 5′-GGGRNYYYCC-3′ (R is any purine, Y is any pyrimidine, and N is any nucleotide), which consists of 5-base pair (bp) 5′ subsite for p50, and 4 bp subsite for p65 (Kunsch et al., 1992; Chen et al., 1998). The nuclear activity of NF-κB is terminated by the newly synthesized IκBα, which enters the nucleus, binds to NF-κB and takes it out into cytoplasm.

NF-κB activating signals converge on the cytoplasmic IκB kinase (IKK), a multiprotein complex that phosphorylates IκBα at serine residues 32 and 36, leading to its ubiquitination at lysine-21 and lysine-22 and then to its rapid degradation by the 26S proteasome (reviewed in Karin, 1999). Native IKK complexes purified from mammalian cells have molecular weight of ~700 kDa, and are composed of the catalytic basic helix–loop–helix-containing kinases IKKα and IKKβ, and a regulatory subunit IKKγ (NEMO) in stoichiometric amounts, whose association is required for coupling IKK to upstream kinases (Yamaoka et al., 1998). Recently, Tangethoff et al. (2003) found that tetrameric oligomerization of IKKγ is obligatory for activity of IKK complex. The activation of IKK kinase is induced by various extracellular signals including tumor necrosis factor-alpha (TNF), interleukin-1 (IL-1) and viral replication (e.g. Respiratory Syncytial Virus, Tian et al., 2002) through complicated, not fully resolved, transduction pathways.

Kinetic studies of IKK indicate that its activity is transient, peaking within minutes of stimulation and rapidly decreasing thereafter. IKK inactivation is controlled by the zinc finger protein termed A20, which like IκBα, is strongly NF-κB responsive (Krikos et al., 1992). Mice deficient in A20 develop severe inflammation and cachexia, are hypersensitive to TNF, and die prematurely (Lee et al., 2000). At a biochemical level, A20-deficient fibroblasts show persistent IKK activation after TNF stimulation demonstrating its essential role in mediating IKK inactivation (Lee et al., 2000). Despite these observations the exact mechanism of A20's action is not fully resolved. There are two main possible hypotheses: A20 may act at the level of IKK, binding to IKKγ, mostly through its C-terminal (zinc finger) region (Zhang et al., 2000); or it may block the upstream transduction pathway between extracellular signal and IKK by binding to TNF receptor associating proteins, interfering with the recruitment of IKK to the activating receptor (Song et al., 1996; He and Ting, 2002, reviewed in Beyaert et al., 2000). Our model is based on the first hypothesis, although it should work reasonably well even if A20 acts by blocking the transduction pathway between an extracellular signal and IKK.

In the present paper, we apply ordinary differential equations (ODEs) to model the NF-κB regulatory network (see Tyson et al., 2003 for a recent review of ODEs modeling). The model constructed includes two regulatory feedback loops; the first involving IκBα and the second involving A20. While IκBα is a NF-κB inducible inhibitor of NF-κB nuclear activity, the action of A20 is more elaborate. A20 being also NF-κB responsive eases termination of IKK activity, which in turn is responsible for IκBα degradation. This implies that A20 acts as an IκBα activator and an NF-κB inhibitor.

The previous attempt to model the IκB—NF-κB signaling module was made by Hoffmann et al. (2002). While the Hoffmann et al. (2002) model concentrates on the interplay between three isoforms of NF-κB inhibitory proteins IκBα and IκBβ and IκBε, our model accounts for IκBα and A20 inhibitory actions, IKK activation and NF-κB regulated synthesis. Using, in part, the Hoffmann et al. (2002) model, we amended it in three main points:

- We refined the considerations on two-compartment kinetics by taking into account the difference between the nuclear and the cytoplasmic volume.
- Fitting our model we made use of Rice and Ernst (1993) data and Carlotti et al. (2000) considerations indicating that unbound IκBα constitutes less than 15% of the total IκBα. Since only one IκBα molecule binds to a NF-κB heterodimer (Li et al., 1998), IκBα is present in less than 15% excess relative to NF-κB. The Hoffmann et al. (2002) fit implies that the amount of IκBα is several times larger than that of NF-κB. Such large quantities of free IκBα substantially alter the IκBα and NF-κB intercompartment kinetics.
- We re-estimated the mRNA transcription and translation coefficients by using constraints following from data on a molecular level. The IκBα inducible mRNA synthesis coefficient used in Hoffmann et al. (2002) model implies the transcription speed of hundreds of mRNA transcripts per second, which is unrealistic.

2. Model formulation

The model proposed involves two-compartment kinetics of IKK, NF-κB, A20, IκBα, their complexes, and mRNA transcripts of A20, IκBα, and of a hypothetical control gene, cgen. The IKK complex, as well as the dimer NF-κB will be considered as single proteins, i.e. the dynamics leading to formation of these complexes will be disregarded.

The regulatory system considered has two activators IKK and NF-κB, and two inhibitors A20 and IκBα. In the presence of an extracellular signal such as TNF or IL-1, IKK is transformed into its active (phosphorylated) form. In this form it is capable of phosphorylating IκBα, which in turn leads to its degradation. In resting cells, the unphosphorylated IκBα binds to NF-κB and sequesters it in an inactive form in the cytoplasm. As a result, degradation of IκBα releases the second activator, NF-κB. The free NF-κB enters the nucleus and upregulates transcription of the two inhibitors IκBα and A20, and of large number of other genes including the control gene cgen. The newly synthesized IκBα again inhibits NF-κB, while A20 inhibits IKK by catalysing its transformation into another inactive form, in which it is no longer capable of phosphorylating IκBα.

2.1. Background: basic processes

The kinetics considered involves formation and dissociation of complexes, catalysis, mRNA synthesis and translation as well as transport between nucleus of volume U and cytoplasm of volume V. Some substrates may exist both in cytoplasm and in the nucleus, and below we use subscript c for cytoplasm and n for nucleus.

1. We assume that the transport rate of a given substrate to or from cytoplasm is proportional to its nuclear or cytoplasmic density, respectively. Let a_c and a_n denote the amount of the substrate, respectively, in cytoplasm and nucleus, while $A_c = a_c/V$ and $A_n = a_n/U$ denote cytoplasmic and nuclear concentrations of the substrate. With lower case letters we will denote amounts, with capital letters molar concentrations. Assuming that the intensity of transport is proportional to the concentration of transported substrate, the pure transport equations can then be written as follows:

$$\frac{da_c}{dt} = -T_c A_c + T_n A_n, \tag{1}$$

$$\frac{da_n}{dt} = -T_n A_n + T_c A_c, \tag{2}$$

where T_n, T_c denote coefficients of cytoplasmic and nuclear export. One may expect that these coefficients are proportional to the area of the nucleus surface S; however, it is not so evident, since the transport proceeds through specialized pores, and the number of these may not be proportional to the nuclear surface area. Let us note that

$$\frac{da_c}{dt} + \frac{da_n}{dt} = 0, \tag{3}$$

which means that when transport only is considered, the total amount of substrate $a_c + a_n$ is constant. Dividing Eqs. (1) and (2), respectively, by V and U, we obtain

$$\frac{dA_c}{dt} = -t_c A_c + t_n A_n, \tag{4}$$

$$\frac{dA_n}{dt} = -k_v t_n A_n + k_v t_c A_c, \tag{5}$$

where $t_c = T_c/V$ and $t_n = T_n/V$ are the scaled coefficients of transport, and $k_v = V/U$. While using the scaled coefficients of transport, one has to remember that their values are volume-dependent, and may be different for different cells. Note that

$$\frac{dA_c}{dt} + \frac{dA_n}{dt} = 0 \tag{6}$$

if and only if $k_v = 1$, i.e. when cytoplasm and nucleus are of the same volume. The Hoffmann et al. (2002) model equations are based on the assumption that the transport conserves the sum of concentrations, an assumption that is only valid if the compartments are of the same volume.

2. Our model includes two inducible genes A20 and IκBα, the transcription rate of which is regulated by NF-κB. Let a_t denote the amount of mRNA transcript of A20 or IκBα. We assume that the transcription rate is a sum of a steady term and of an inducible term, the latter proportional to nuclear concentration of NF-κB, which implies

$$\frac{da_t}{dt} = C_0 + C_1\, NF\kappa B_n - c_2 a_t. \tag{7}$$

Hoffmann et al. (2002) assumed that the transcription of IκBα isoform is a second-order process proportional to the square of NF-κB concentration, arguing that NF-κB is a dimer and as a dimer it can be assumed to bind DNA in a nonlinear, cooperative fashion. In our opinion, the quadratic term would be justified if the gene promotory region had two NF-κB binding sites, and binding to both of them would be necessary to regulate the transcription. In any case, Hoffmann et al. (2002) found that the assumed nonlinearity is not essential for qualitative behavior of the model. The mRNA transcript is produced in the nucleus but since, prior to the translation, it is transported to the cytoplasm, its concentration is calculated using the cytoplasmic volume, i.e. $A_t = a_t/V$, and we have

$$\frac{dA_t}{dt} = c_0 + c_1\, NF\kappa B_n - c_2 A_t, \tag{8}$$

where $c_0 = C_0/V$, $c_1 = C_1/V$ are the scaled coefficients.

We assume that the translation rate per unit volume is proportional to cytoplasmic transcript concentration.

3. In addition to the spontaneous degradation, for which the degradation rate is proportional to the amount of degrading substrate, we consider the

catalysed degradation of cytoplasmic IκBα in complexes with IKKa. The active IKK may phosphorylate IκBα, which leads to its ubiquitination at lysine-21 and lysine-22 and then to its degradation by the 26S proteasome. Following Hoffmann et al. (2002) we assume that the complex (IKKa|IκBα) degrades (with degradation rate proportional to its amount) and as a result the free IKKa is regained, but IκBα is lost. The same we assume for the (IKKa|NF-κB|IκBα) complexes, the degradation of which frees NF-κB and IKKa, but again, IκBα is lost. Hoffmann et al. (2002) assumed that ubiquitination and proteolysis immediately follow IκBα phosphorylation. However, we expect, that in reality, both ubiquitination and proteolysis may take several minutes, which slows down freeing and nuclear translocation of NF-κB. This conjecture is supported by Yang et al. (2003, Fig. 6A) measurements showing existence of a pool of phosphorylated IκBα appearing 8 min after IL-1β stimulation. This is why we will modify the NF-κB nuclear transport coefficient taking into account the time needed for ubiquitination and proteolysis. We can make such a correction, since according to the rest of the model, all free cytoplasmic NF-κB results from degradation of (IKKa|NF-κB|IκBα) complexes. Without this correction, one obtains an extremely rapid build-up of NF-κB. As a result, Hoffmann et al. (2002), to fit their data, had to assume that concentration of free IκBα is much larger than that of NF-κB, which results in slowing down the nuclear build-up of NF-κB, but is in apparent opposition to Rice and Ernst (1993) measurements.

2.2. Kinetics of activation and inactivation of IKK

It is assumed that the cytoplasmic complex IKK may exist in one of three forms:

- neutral (denoted by IKKn), which is specific to resting cells without any extracellular stimuli like TNF or IL-1,
- active (denoted by IKKa)
- inactive, but different from the neutral form, possibly overphosphorylated (denoted by IKKi).

Activity of the IKK kinase may be induced by various extracellular signals including TNF, IL-1 and various viruses through complicated and not fully resolved transduction pathways. It coincides with serine phosphorylation of IKKα and IKKβ and with serine/threonine phosphorylation of IKKγ. However, IKKα and IKKβ are not functionally equivalent. Only the phosphorylation of IKKβ is required for IKK activation by TNF or IL-1. The basic role of IKKα in NF-κB signaling is different, it enters the nucleus and in conjunction with RelA is recruited to NF-κB responsive promoters (Yamamoto et al., 2003; Anest et al., 2003). Activation of IKKβ results from phosphorylation of two serine residues 177 and 181 in the activation T-loop, and serine to alanine mutations in both of these sites abolish IKK activation upon TNF and IL-1 stimulation (Delhase et al., 1999) or upon Tax-directed phosphorylation (Carter et al., 2001). Upon TNF stimulation, the transformation from neutral IKK (IKKn) to active IKK is very rapid and after 2 min one may observe an increase in IKK activity (Delhase et al., 1999, Fig. 1A).

Further phosphorylation transforms the active IKKβ into the low-activity form (in our model considered as inactive, IKKi). In this form (in addition to the 177 and 181 serines) the 9 or 10 COOH-terminal serines are phosphorylated, the interaction between COOH-terminal activation domain and the kinase domain is weakened, and the activity of IKK decreases (Delhase et al., 1999, Fig. 5). Since the mutations in the 177 and 181 serine residues completely prevent IKKβ phosphorylation, Delhase et al. (1999) concluded that phosphorylation of COOH-terminal serines is mostly autophosphorylation, which can only follow the T-loop phosphorylation. However, it was not verified directly (by switching the TNF signal off) whether or not TNF enhances the COOH-terminal serine phosphorylation. In the model proposed, we will follow the Delhase et al. (1999) observation, and assume that IKK can only be transformed into IKKi form from the IKKa form. We also assume that the transformation rate from IKKa to IKKi is, in part, independent of TNF.

Another crucial assumption we make is that the transformation from IKKa to IKKi is triggered by the cytoplasmic protein A20. This assumption follows from a series of observations. First, Lee et al. (2000) observed that A20 is needed to terminate NF-κB's presence in the nucleus. They found, that in A20-deficient ($A20^{-/-}$) mouse embryonic fibroblasts (MEFs), once NF-κB enters the nucleus it remains there at a constant level for at least 3 h. Since they also observed a high level of mRNA IκBα transcript together with no free IκBα in the cytoplasm, they concluded that in $A20^{-/-}$ cells the IKK activity is persistent in contrast to wild-type cells. The direct measurement of IKK activity in lysates from $A20^{-/-}$ MEFs confirms this suggestion. In support of this observation, Arvelo et al. (2002, Fig. 3) found that the overexpression of A20 in HepG2 cells inhibits IκBα degradation 15 min from the beginning of TNF stimulation. The second observation comes from Zhang et al. (2000) who found that A20 may bind directly to IKKγ. The binding occurs both through its N-terminal and even more effectively, through its C-terminal (zinc finger) region. Zhang et al. (2000) found that A20, while lowering the IKK kinase activity (i.e. inhibiting the IκBα phosphorylation), also augments IKK phosphorylation. Specifically, Delhase et al. (1999) and Zhang et al. (2000) have shown that the termination of IKK activity is due

to its transformation into an inactive form, a species different from the neutral form in resting cells.

It is not resolved whether A20 eases termination of IKK activity after TNF and IL-1 stimulation, or solely after TNF stimulation. Lee et al. (2000, Fig. 3F) found that A20 is not important in termination of IKK and NF-κB activity upon IL-1 stimulation. In contrast, Song et al. (1996, Fig. 5) showed that NF-κB-dependent luciferase activity decreases after either TNF or IL-1 stimulation with increasing concentration of the A20 expression vector.

The remaining assumptions we make regarding IKK kinetics, are:

- IKKn is synthesized "de novo" with some synthesis rate k_{prod}.
- Each form of IKK, i.e. IKKn, IKKa and IKKi, undergoes degradation with the same degradation rate k_{deg}.
- IKKa can form transient complexes with IκBα proteins or (IκBα|NF-κB) complexes. Formation of these complexes leads to IκBα phosphorylation, ubiquitination and degradation in proteasome. The assumed IKK kinetics is depicted in Fig. 1.

2.3. Two-compartment kinetics of A20, IκBα and NF-κB

In this part of the model we partially make use of the Hoffmann et al. (2002) model of the IκB–NF-κB signaling module. While Hoffmann et al. (2002) analysed the interplay between the three isoforms of NF-κB inhibitory proteins IκBα, IκBβ, and IκBε, we focus on IκBα, postponing the inclusion of the other two to a future study. More precisely, we approximate the collective action of these three isoforms by the action of the most active and abundant inhibitor, i.e. IκBα, the knockout of which, in contrast to the other two isoforms, is lethal (Gerondakis et al., 1999, and references therein).

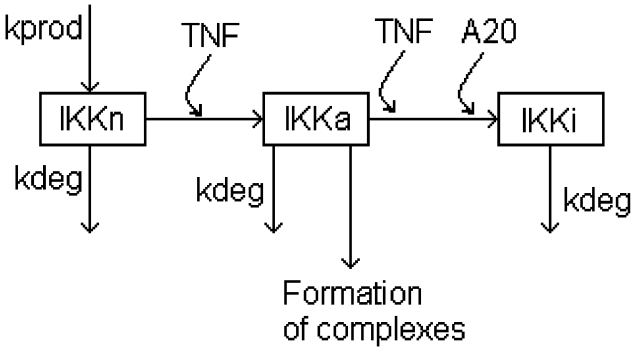

Fig. 1. Transient activation of IKK. Upon TNF stimulation, neutral IKKn is transformed into its active form IKKa, which forms the complexes with IκBα and (IκBα|NF-κB). Transformation from active form IKKa to IKKi is enhanced by the A20 and TNF. IKKn is synthesized de novo with synthesis rate k_{prod}, while each form of IKK, i.e. IKKn, IKKa and IKKi, undergoes degradation with the same degradation rate k_{deg}.

In resting cells, almost all NF-κB is sequestered in complexes with IκBα in cytoplasm. According to Rice and Ernst (1993), IκBα is less than 15% in excess relative to NF-κB, while Carlotti et al. (2000) conclude that the pool of free IκBα is of the order of 10% of total IκBα and it is distributed between the nucleus and cytoplasm. The ratio of free IκBα nuclear-import/nuclear-export rates was estimated by Carlotti et al. (2000) to be equal to 2, which is supported also by experiments by Yang et al. (2001, Fig. 1), where upon gross overexpression of IκBα-EGFP, when IκBα is likely to be present largely free of NF-κB, the ratio of nuclear to cytoplasmic fluorescence is of the order of 2–3. Note that the ratio of import/export rates corresponds to the ratio of nuclear to cytoplasmic concentrations (which can be measured in fluorescence experiments), rather than to the ratio of nuclear and cytoplasmic amounts, which depends both on concentrations and compartment volumes. In resting wild-type cells, IκBα is observed only in the cytoplasm where it remains bound to NF-κB, not in the nucleus (Rodriguez et al., 1999, Fig. 3), which also confirms that the pool of free IκBα is relatively small.

As already stated, upon the TNF stimulation IKK is transformed into its active form IKKa, and in this form it forms complexes with IκBα and (IκBα|NF-κB), which leads to IκBα phosphorylation, ubiquitination, and degradation. The free NF-κB rapidly enters the nucleus where it may bind to specific κB sites in the A20 and IκBα promoters and activate their expression. The newly synthesized A20 enhances IKK inhibition, while the newly synthesized IκBα enters the nucleus, binds to NF-κB and takes it out into cytoplasm. Then the cycle may be repeated, but since the IKK activity is already lowered by A20, the amplitude of the subsequent cycles is smaller.

The first cycle takes about 1 h, the following ones are longer. The first active IKK appears after 2 min of TNF stimulation (Delhase et al., 1999, Fig. 1A), the degradation of cytoplasmic (IκBα|NF-κB) takes several minutes and after 10 min the free NF-κB is present in the nucleus (Hoffmann et al., 2002, Fig. 2E). The peak of IKK activity is attained after 10–15 min from the beginning of stimulation (Delhase et al., 1999, Fig. 1A; Lee et al., 2000, Fig. 3E), at the peak the large fraction of all of IKK is in its active form. Then A20, the mRNA transcript of which is rapidly synthesized upon NF-κB activation (Lee et al., 2000, Fig. 2D), inhibits IKK activity by accelerating its transformation into the inactive form IKKi. Since the difference between wild-type and $A20^{-/-}$ cells (A20−/−) is visible 30 min after the beginning of TNF stimulation (Lee et al., 2000, Fig. 2E), we can deduce that the translation of A20 also proceeds rapidly. The IκBα synthesis and translation are also rapid. After synthesis IκBα enters the nucleus and

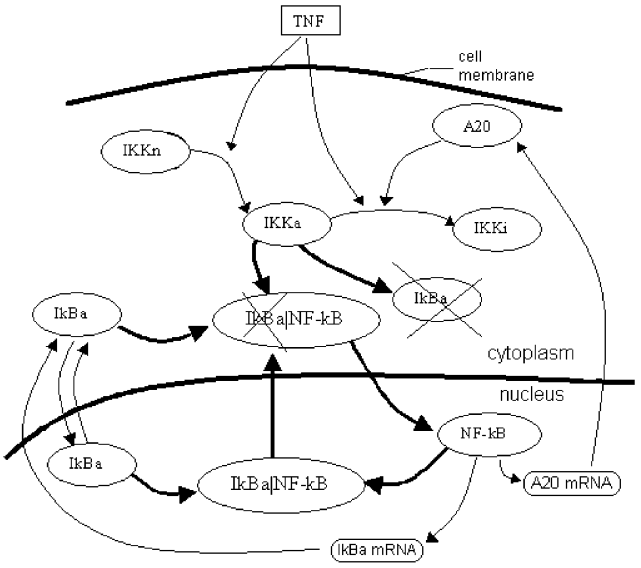

Fig. 2. Schematic depiction of the model. Upon TNF stimulation, neutral IKKn is transformed into its active form IKKa. Active IKKa forms complexes with IκBα and (IκBα|NF-κB), and strongly catalyses IκBα degradation. Liberated NF-κB enters the nucleus where it binds to κB motifs in A20, IκBα or other gene promoters. The newly synthesized IκBα enters the nucleus and leads NF-κB again to cytoplasm, while newly synthesized A20 triggers transformation of IKKa into inactive IKKi. The bold arrows stand for very fast dynamics, with characteristic time-scales of a minute or shorter.

leads NF-κB into cytoplasm. After 60–75 min, almost no NF-κB is left in the nucleus. The complete kinetics of the model is depicted in Fig. 2.

Note that the NF-κB kinetics would be quite different, if initially there was a large pool of free IκBα in the nucleus. In this case, the entering NF-κB would rather bind to nuclear portion of IκBα, and then the (IκBα|NF-κB) complexes would be shuttled out of the nucleus into cytoplasm, where IκBα would be again degraded. This would imply that the typical NF-κB molecule would have to circulate between cytoplasm and nucleus until there is no (or little) IκBα in the nucleus.

2.4. Equations

In this section, we give and discuss the equations of the model following the assumed kinetics. Upper-case letters denote molar concentration of molecules and their complexes. Nuclear concentration is represented by subscript n, while the subscript c denoting concentration of substrate in the cytoplasm is now omitted, to simplify the notation. Concentration of the mRNA transcript of A20, IκBα and cgen is denoted by subscript t.

Notation guide:

- *IKKn*—cytoplasmic concentration of neutral form of IKK kinase,
- *IKKa*—cytoplasmic concentration of active form of IKK,
- *IKKi*—cytoplasmic concentration of inactive form of IKK,
- $I\kappa B\alpha$—cytoplasmic concentration of IκBα,
- $I\kappa B\alpha_n$—nuclear concentration of IκBα,
- $I\kappa B\alpha_t$—concentration of IκBα mRNA transcript calculated per cytoplasmic volume V,
- $(IKKa|I\kappa B\alpha)$—cytoplasmic concentration of complexes of IKKa and IκBα,
- $(NF\kappa B_n|I\kappa B\alpha_n)$—nuclear concentration of complexes of NF-κB and IκBα, notation for the remaining complexes is analogous (we will write NFκB instead NF-κB in equations),
- T_R—logical variable, $T_R = 1$ if signal (e.g. TNF or IL-1) is present, $T_R = 0$ if no signal is present,
- $k_v = V/U$—the ratio of cytoplasmic and nuclear volumes.

IKK in the neutral state IKKn: The first term describes IKKn synthesis "de novo", the second describes degradation, while the last one depletion of IKKn d ue to its signal-induced transformation into active form IKKa:

$$\frac{\mathrm{d}}{\mathrm{d}t} IKKn(t) = k_{prod} - k_{deg}\, IKKn(t) - T_R k_1\, IKKn(t). \quad (9)$$

IKK in the active state IKKa: The first two lines represent formation of IKKa from IKKn upon the signal activation, depletion of IKKa, due to transformation into inactive form IKKi, spontaneous and induced by A20, and its degradation. We assumed that the signal ($T_R = 1$) is needed for the catalytic action of A20 and that this action is proportional to the density of A20, without any saturation. This assumption is justified by the observation of Song et al. (1996), who found that NF-κB luciferase decreases monotonically with the concentration of A20 expression vector increasing 30-fold. The third and fourth lines describe depletion of free IKKa due to formation of complexes (IKKa|IκBα) and its recovery after catalytic degradation of these complexes. The fifth and sixth lines represent changes in IKKa concentration due to formation and catalytic degradation of trimolecular complexes

$$\begin{aligned}\frac{\mathrm{d}}{\mathrm{d}t} IKKa(t) = {} & T_R k_1\, IKKn(t) - k_3\, IKKa(t) \\ & - T_R k_2\, IKKa(t)\, A20(t) \\ & - k_{deg}\, IKKa(t) - a_2\, IKKa(t)\, I\kappa B\alpha(t) \\ & + t_1 (IKKa|I\kappa B\alpha)(t) \\ & - a_3\, IKKa(t)(I\kappa B\alpha|NF\kappa B)(t) \\ & + t_2 (IKKa|I\kappa B\alpha|NF\kappa B)(t). \end{aligned} \quad (10)$$

IKK in the inactive state IKKi: The first two terms correspond to the formation of inactive IKKi from IKKa upon spontaneous inactivation and the catalytic action of A20, while the third term describes

degradation:

$$\frac{\mathrm{d}}{\mathrm{d}t} IKKi(t) = k_3\, IKKa(t) + T_R k_2\, IKKa(t)\, A20(t) - k_{deg}\, IKKi(t). \quad (11)$$

IKKa|IκBα complexes: Equation represents formation of (IKKa|IκBα) complexes and their degradation. Protein IκBα is catalytically degraded due to phosphorylation caused by IKKa, while free IKKa is recovered (see the fourth line of Eq. (10)):

$$\frac{\mathrm{d}}{\mathrm{d}t}(IKKa|I\kappa B\alpha)(t) = a_2\, IKKa(t)\, I\kappa B\alpha(t) - t_1(IKKa|I\kappa B\alpha)(t). \quad (12)$$

(IKKa|IκBα|NF-κB) complexes: Described by their formation due to association between IKKa and (IκBα|NF-κB) complexes and degradation due to catalytic activity of IKKa:

$$\frac{\mathrm{d}}{\mathrm{d}t}(IKKa|I\kappa B\alpha|NF\kappa B)(t) = a_3\, IKKa(t)(I\kappa B\alpha|NF\kappa B)(t) - t_2(IKKa|I\kappa B\alpha|NF\kappa B)(t). \quad (13)$$

Free cytoplasmic NF-κB: The first line represents liberation of free NF-κB due to dissociation of (IκBα|NF-κB) complexes and its depletion due to formation of these complexes. The second line accounts for liberation of NF-κB due to the catalytic activity of IKKa. The last line describes transport of free cytoplasmic NF-κB to the nucleus:

$$\frac{\mathrm{d}}{\mathrm{d}t} NF\kappa B(t) = c_{6a}(I\kappa B\alpha|NF\kappa B)(t) - a_1 NF\kappa B(t)\, I\kappa B\alpha(t) + t_2(IKKa|I\kappa B\alpha|NF\kappa B)(t) - i_1\, NF\kappa B(t). \quad (14)$$

Free nuclear *NF-κB*: The first term describes transport into the nucleus adjusted to the nuclear volume by the coefficient $k_v = V/U$. The second term represents depletion of free NF-κB due to the association with nuclear IκBα:

$$\frac{\mathrm{d}}{\mathrm{d}t} NF\kappa B_n(t) = i_1 k_v\, NF\kappa B(t) - a_1\, I\kappa B\alpha_n(t)\, NF\kappa B_n(t). \quad (15)$$

A20 protein: Described by its mRNA synthesis and constitutive degradation:

$$\frac{\mathrm{d}}{\mathrm{d}t} A20(t) = c_4\, A20_t(t) - c_5\, A20(t). \quad (16)$$

A20 transcript: As already stated, the concentration of the transcripts is calculated using the cytoplasmic volume. The first term stands for constitutive A20 mRNA synthesis and the second term for NF-κB inducible synthesis, while the last term describes degradation of the transcript:

$$\frac{\mathrm{d}}{\mathrm{d}t} A20_t(t) = c_2 + c_1\, NF\kappa B_n(t) - c_3\, A20_t(t). \quad (17)$$

Free cytoplasmic IκBα protein: The first line accounts for association with IKKa and NF-κB, respectively. The second line describes formation of the IκBα protein due to the mRNA synthesis and the constitutive degradation of IκBα. The last line represents transport into and out of the nucleus:

$$\frac{\mathrm{d}}{\mathrm{d}t} I\kappa B\alpha(t) = -a_2\, IKKa(t)\, I\kappa B\alpha(t) - a_1\, I\kappa B\alpha(t)\, NF\kappa B(t) + c_{4a}\, I\kappa B\alpha t(t) - c_{5a}\, I\kappa B\alpha(t) - i_{1a}\, I\kappa B\alpha(t) + e_{1a}\, I\kappa B\alpha_n(t). \quad (18)$$

Free nuclear IκBα protein: The first term corresponds to the association with nuclear NF-κB, and the other terms represent the transport into and out of the nucleus adjusted for nuclear volume by the coefficient k_v:

$$\frac{\mathrm{d}}{\mathrm{d}t} I\kappa B\alpha_n(t) = -a_1\, I\kappa B\alpha_n(t)\, NF\kappa B_n(t) + i_{1a} k_v\, I\kappa B\alpha(t) - e_{1a} k_v\, I\kappa B\alpha_n(t). \quad (19)$$

IκBα transcript: The first term stands for constitutive IκBα mRNA synthesis and the second term for inducible synthesis, while the last term describes degradation of transcript:

$$\frac{\mathrm{d}}{\mathrm{d}t} I\kappa B\alpha_t(t) = c_{2a} + c_{1a}\, NF\kappa B_n(t) - c_{3a}\, I\kappa B\alpha_t(t). \quad (20)$$

Cytoplasmic (IκBα|NF-κB) complexes: The first line describes formation of the complexes due to IκBα and NF-κB association and their subsequent degradation. The first term in the second line represents depletion of the (IκBα|NF-κB) complexes due to the catalytic activity of IKKa. The last term represents transport of the complex from the nucleus:

$$\frac{\mathrm{d}}{\mathrm{d}t}(I\kappa B\alpha|NF\kappa B)(t) = a_1\, I\kappa B\alpha(t) NF\kappa B(t) - c_{6a}(I\kappa B\alpha|NF\kappa B)(t) - a_3 IKKa(t)(I\kappa B\alpha|NF\kappa B)(t) + e_{2a}(I\kappa B\alpha_n|NF\kappa B_n)(t). \quad (21)$$

Nuclear (IκBα|NF-κB) complexes: Described by their formation due to IκBα and NF-κB association and their transport out of the nucleus adjusted for the nuclear volume:

$$\frac{\mathrm{d}}{\mathrm{d}t}(I\kappa B\alpha_n|NF\kappa B_n)(t) = a_1\, I\kappa B\alpha_n(t)\, NF\kappa B_n(t) - e_{2a} k_v (I\kappa B\alpha_n|NF\kappa B_n)(t). \quad (22)$$

Control gene transcript: The first term stands for constitutive cgen mRNA synthesis and the second term for inducible synthesis, while the last describes

degradation of transcript:

$$\frac{\mathrm{d}}{\mathrm{d}t} cgen_t(t) = c_{2c} + c_{1c}\, NF\kappa B_n(t) - c_{3c}\, cgen_t(t). \quad (23)$$

Hoffmann et al. (2002) also took into account spontaneous dissociation of (IκBα|NF-κB) complexes, association between (IKKa|IκBα) and NF-κB, and transport of free NF-κB out of the nucleus. We found that these processes have no significant impact on dynamics studied and we disregard them to simplify the model.

3. Results

To validate the proposed model, we analysed its ability to reproduce the data from Lee et al. (2000) and Hoffmann et al. (2002) experiments on mouse fibroblasts. Lee et al. (2000) measured the response of wild-type and A20-deficient cells to a persistent TNF signal. For both types of cells, Lee et al. collected data on IκBα mRNA, cytoplasmic IκBα, NF-κB, IKKβ (the key component of IKK) and IKK kinase activity, this latter estimated in an immunoprecipitation-kinase assay using GST-IκBα as a substrate. Additionally, for wild-type cells, they measured A20 mRNA levels. Hoffmann et al. (2002) measurements involve wild-type cells, and cells with knockout of one or two of the IκB isoforms (IκBα, IκBβ, IκBε). Since in our approximate model IκBα represents all these isoforms, we use only his data on wild-type cells for persistent and pulse-like TNF activation. We will compare our predictions with his measurements of NF-κB, for persistent TNF activation and pulse-like activation for 15 and 60 min, and of cytoplasmic IκBα for persistent TNF activation. The most important data we miss is the evolution of the level of protein A20. The protein is probably unstable, or catalytically degraded and thus hard to measure. We also have no information on the very unstable bi- and trimolecular complexes containing IKK, but since these complexes are short-lasting their molar densities are relatively small. It follows from the model that NF-κB is either free in the nucleus, or it is sequestered in cytoplasmic complexes with IκBα. The reason is that the free cytoplasmic NF-κB either quickly binds to IκBα or it quickly enters the nucleus, while (IκBα|NF-κB) complexes are shuttled out of the nucleus. Nevertheless, the additional data on molar concentration of cytoplasmic and nuclear (IκBα|NF-κB) complexes will eventually verify this hypothesis. Despite the fact that this additional data could remove the ambiguities of the model, the data already collected enable us to trace the time behavior of majority of the most important variables in the pathway considered.

Because of a large number of undetermined parameters, model fitting is not easy. We decided to carry out the fit "manually" rather than to try to quantify the data, which is in the form of blots, and then to apply one of the fitting engines available. The first reason is that such quantification is by no means unique, the second is that when fitting, we have to take into account diverse, usually not precise, information coming from different researchers and our own intuitive understanding of the process. We applied the following fitting method:

(1) Start from a reasonable set of parameters, which produces a correct steady state in the absence of TNF signal.
(2) Proceed with the signal initiated by TNF along the autoregulation loop.
(3) Iterate item 2 until the fit to all the data is satisfactory.

The observation (Rice and Ernst, 1993) that in resting cells there is no more than 15% of all IκBα, which is not complexed with NF-κB imposes the upper bound on IκBα mRNA constitutive synthesis coefficients c_{2a}. We set $c_{2a} = 0$, which gives roughly 5% excess of IκBα with respect to NF-κB. On a first glimpse it may be surprising that no constitutive IκBα synthesis is needed for NF-κB inhibition in resting cells. However, in fact, if there is not enough IκBα to sequester NF-κB in the cytoplasm, some of NF-κB enters the nucleus and triggers IκBα synthesis, up to the point when amount of IκBα is sufficient to keep most of NF-κB in cytoplasm. In the resting cells, this autoregulation is so efficient that even after lowering the coefficient of IκBα inducible synthesis ten-fold from "the best fit value", the total amount of IκBα remains almost unchanged and still over 90% of NF-κB is sequestered by IκBα.

The TNF signal first causes IKK activation (e.g. transformation of IKKn into IKKa), and as a result the activated IKKa initiates degradation of cytoplasmic (IκBα|NF-κB) and of a small pool of cytoplasmic IκBα, enabling the free NF-κB to enter the nucleus. Once NF-κB builds up in the nucleus it upregulates the transcription of the A20 and IκBα genes. As stated in item 2, we first fit the coefficients regulating IKK activation (using the Lee et al. (2000) data on IKK activity), then the coefficients regulating the cytoplasmic (IκBα|NF-κB) and IκBα degradation and so forth.

If there were no feedback loops in the pathway, the proposed method would be quite efficient, but since they exist it is necessary to iterate the signal tracing several times, until the fit is satisfactory. It is not obvious whether the method, in general, converges, but it seems so, provided we start from a relatively accurate set of parameters and provided that the model approximates the true regulatory mechanism reasonably well.

It is not easy to find a fitting set of parameters, but once the satisfactory fit is found, it is not difficult to find other sets which are almost equivalent. This ambiguity is mostly caused by the lack of measurements of absolute

values of protein or mRNA concentrations. The data at our disposal only trace the time behavior expressed in arbitrary units. The action exerted by some components of the model onto the rest of the pathway is determined by their concentration multiplied by undetermined coupling coefficients. Hence, once we have a good fit, we may obtain another one, using a smaller coupling coefficient and a proportionately larger absolute level. For example, the average level of A20 protein is governed by a score of coefficients, and so having no independent data on these coefficients we can set the level high or low, and then tune parameter k_2 so as to adjust the action of A20 protein to a right level. There also exist single parameters, the value of which can be changed in a very broad range without a significant influence on the time behavior of any substrate or complex the data for which are at our disposal.

3.1. The details of numerical solution

Since we observe both slow and fast dynamics in the model, and some variables (like IKKa|IκBα) have very sharp kinks, a good solver is essential. Moreover, to carry out the parameter fitting one has to run the program many times. The fourth-order MATLAB solver was found to be an efficient tool. The time behavior of all 15 variables is presented in Figs. 3 and 4. All the plots correspond to the parameter values in Tables 1–4 in the Appendix. The simulation was performed for wild-type cells, in which all genes were active. To reach the resting cell equilibrium state, we start the simulation 101 h prior to the signal being turned on. The last hour of this stage is shown.

At $t = 1$ h the rectangular TNF signal is turned on for 6 h to the end of the simulation time, Fig. 3A. In the resting phase, there is only IKK in the neutral non-active state IKKn. Under the TNF signal, IKKn is quickly transformed into the active state IKKa and then into the inactive state IKKi. The persistent TNF activation causes a pulse activation of IKK, followed by a relatively low tail, Fig. 3C. As we will see, even this "tail" activity is high enough to influence the rest of the pathway. The pulse of IKKa initiates the cascade. First, (Fig. 3E) the small pool of free cytoplasmic IκBα, and (Fig. 3F) cytoplasmic complexes (IκBα|NF-κB) are degraded. The released NF-κB leads out the small pool of free nuclear IκBα (Fig. 3G) and then builds up in the nucleus (Fig. 3H). Since there is much more entering NF-κB than nuclear IκBα, the evacuation of (IκBα|NF-κB) complexes out of nucleus causes only the small delay in the NF-κB nuclear build-up. The nuclear NF-κB upregulates mRNA expression of both IκBα and A20 (Figs. 3I and J). The peaks in IκBα and A20 transcript level, at 47 min from the beginning of TNF stimulation, are followed by peaks (at 53 and 82 min) in the corresponding free cytoplasmic protein concentrations (Figs. 3E and K). The newly synthesized IκBα enters the nucleus (Fig. 3G) and leads almost all

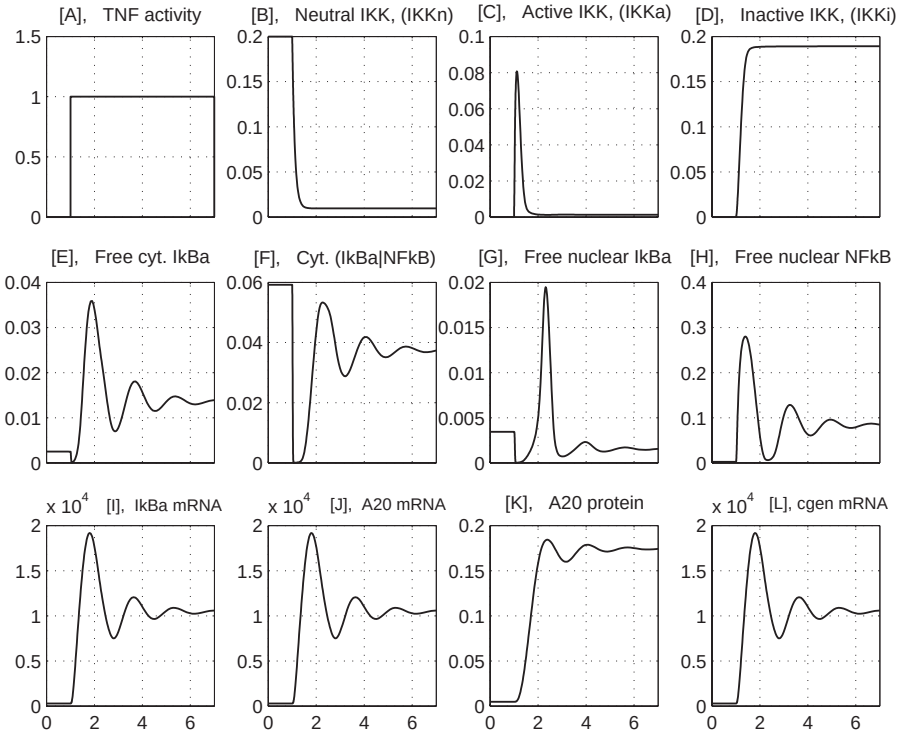

Fig. 3. Numerical solution corresponding to wild-type cells. Persistent TNF activation starts at 1 h. Concentrations (vertical axis) are given in μM, while time (horizontal axis) is in hours. See the text for description of time evolution of the corresponding variables.

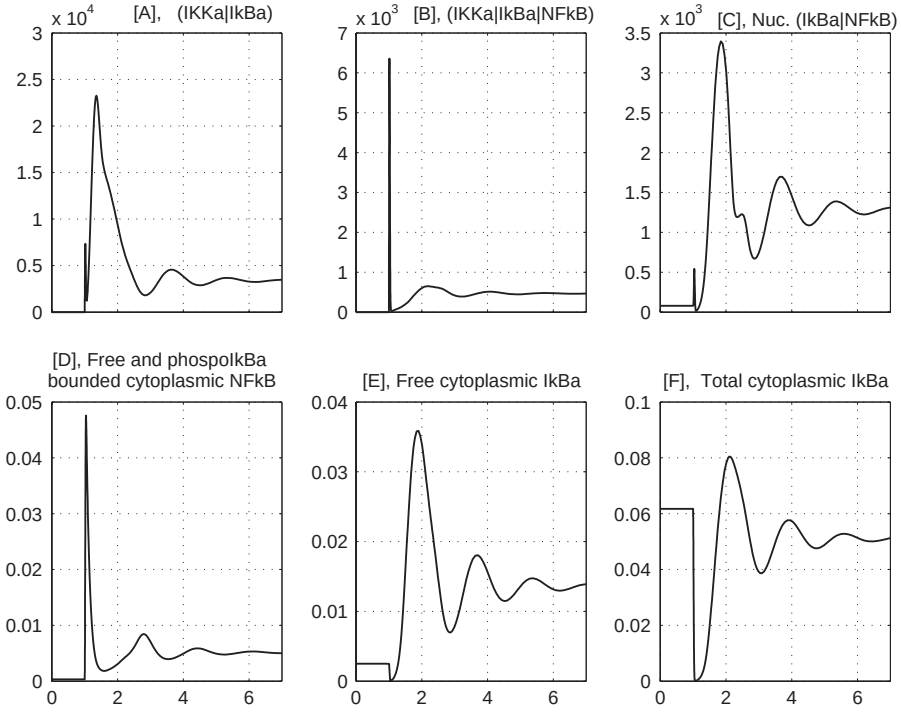

Fig. 4. Numerical solution corresponding to wild-type cells, continued from Fig. 3. Persistent TNF activation starts at 1 h. See text for description of time evolution of the corresponding variables.

NF-κB out of it (Fig. 3H), while A20 triggers IKK inactivation. The IKK inactivation may also proceed independently of A20, but A20 makes this inactivation more efficient, which decreases the level of IKKa.

In Fig. 4, we show the dynamics of the four last variables the time behavior of which is quite different from those in Fig. 3. The corresponding concentrations are also in general lower. The concentrations of (IKKa|IκBα) (Fig. 4A) and (IKKa|IκBα|NF-κB) (Fig. 4B) are small because the phosphorylation of IκBα proceeds very fast and these complexes are unstable. There is also little of the nuclear (IκBα|NF-κB) (Fig. 4C), because these complexes are effectively transported out of nucleus, so their nuclear concentration is small when compared to the cytoplasmic concentration. In Fig. 4D, the free and phospho-IκBα bound cytoplasmic NF-κB is shown. In fact, the free NF-κB almost immediately enters the nucleus, but according to our consideration (see Section 2.1) there is some pool of NF-κB, which is bounded to already phosphorylated, but not yet ubiquitinated or fully degraded IκBα. This explains the narrow high peak in Fig. 4D. In Figs. 4E and F, we show the free and total cytoplasmic IκBα, the last being the sum of free and NF-κB bounded IκBα. Since IκBα is stripped of NF-κB before blotting, the total cytoplasmic IκBα is measured in Western blots expression analysis and thus must be used for fitting. In contrary to IκBα in Lee et al. (2000) and Hoffmann et al. (2002) experiments, NF-κB is assayed by electrophoretic mobility shift assay (EMSA). In this method one measures the amount of DNA-bound NF-κB, which is expected to be proportional to the amount of free NF-κB.

It is worthwhile to note that upon a persistent TNF stimulation, for this specific choice of parameter values, the system asymptotically stabilizes in its single steady state at which nuclear free NF-κB concentration equals 0.084 μM. This implies that 28% of all NF-κB remains free in the nucleus. This concentration of NF-κB results in 1.05×10^{-4} μM asymptotic concentration of the mRNA of the control gene.

3.2. The fits

Typical experimental data at our disposal consist of measurements made in time points that are not uniformly distributed. The non-uniform distribution reflects the fact that during the first hour the oscillations are more rapid and more measurements are needed to accurately trace the dynamic. Therefore, to compare our solutions with experimental data, we rescale the time coordinate, i.e. we calculate the values of corresponding functions in the same time points as in the experiment, and then to guide the eye we connect the resulting discrete points by straight-like segments, thus obtaining a saw-like graph. As already stated, the data were obtained from studies of mouse fibroblasts by two independent experimental groups. Despite the fact that

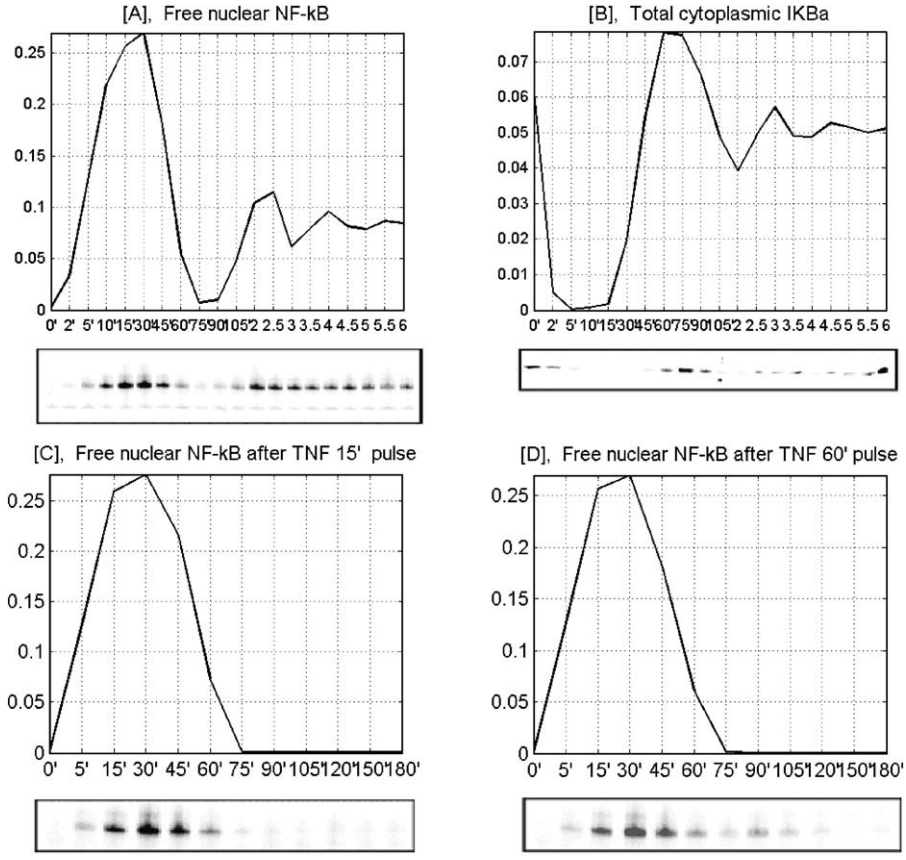

Fig. 5. Model predictions versus Hoffmann et al. (2002) measurements on wild-type cells. The time coordinate is rescaled, and the values of corresponding functions are calculated based on fitted parameters, at the same time points as in the experiment. NF-κB was assayed by EMSA. Concentrations are given in μM. (A) NF-κB during persistent 6 h-long TNF stimulation. (B) Cytoplasmic IκBα protein from the same experiment. (C) NF-κB at and after 15 min-long TNF stimulation. (D) NF-κB at and after 60 min-long TNF stimulation.

there are some discrepancies in their results, we decided to fit the model to these two sets of data using the same set of parameters, see Tables 1–3 in Appendix.

First, let us focus on the Hoffmann et al. (2002) experiments on wild-type cells. In Fig. 5A, we compare our prediction with data on NF-κB (Hoffmann et al., 2002, Fig. 2E), assayed by (EMSA), during persistent 6 h long TNF activation, while in Fig. 6B we show our fit for the cytoplasmic IκBα protein from the same experiment. Both fits seem almost perfect during the first two hours. Subsequently, it seems that the oscillations predicted by our model have a slightly shorter period, and in the case of cytoplasmic IκBα also a smaller amplitude. In Figs. 5C and D we have data (Hoffmann et al., 2002, Fig. 3) on nuclear NF-κB but with the TNF signal lasting for 15 and 60 min, respectively. The pulse of NF-κB lasts for about 1 h both for 15 and 60 min long TNF activation, which well agrees with our predictions. This somehow surprising effect is due to the pulse-like activation of IKK. Termination of this activation is in large part independent of the TNF signal.

Now, let us concentrate on the Lee et al. (2000) data on both wild-type and $A20^{-/-}$ cells. The $A20^{-/-}$ cells are simulated by setting A20 mRNA synthesis coefficient to zero, $c_1 = 0$. In Fig. 6A we depict data (Lee et al., 2000, Fig. 2D) on the A20 mRNA transcript, indicating that, in accordance with the model, A20 is a fast, highly inducible gene. In Fig. 6B we show that the amount of IKK measured by immunoprecipitation by IKKγ antibody remains almost constant. This agrees with our predictions: Since we assume the same degradation constants for all three IKK forms, their summary concentration IKKn + IKKa + IKKi remains also constant, for both type of cells. In Figs. 6C and D we depict data from Lee et al. (2000, Fig. 3E) on IKK kinase activity for wild-type cells (Fig. 6C) and $A20^{-/-}$ cells (Fig. 6D) assessed using the GST-IκBα substrate. Since in our model the only active form of IKK is IKKa, we compare this pulse of activity with the profile of IKKa molar concentration. The fit seems perfect for wild-type cells, while for $A20^{-/-}$ cells our model misses the 30 min minimum, which may suggest existence of some other unresolved regulatory mechanisms. However, the main difference between wild-type and $A20^{-/-}$ cells, which is in the level of activation in the tail following the peak, is well predicted by the model. As we will see in Fig. 7 this difference in IKK activity is

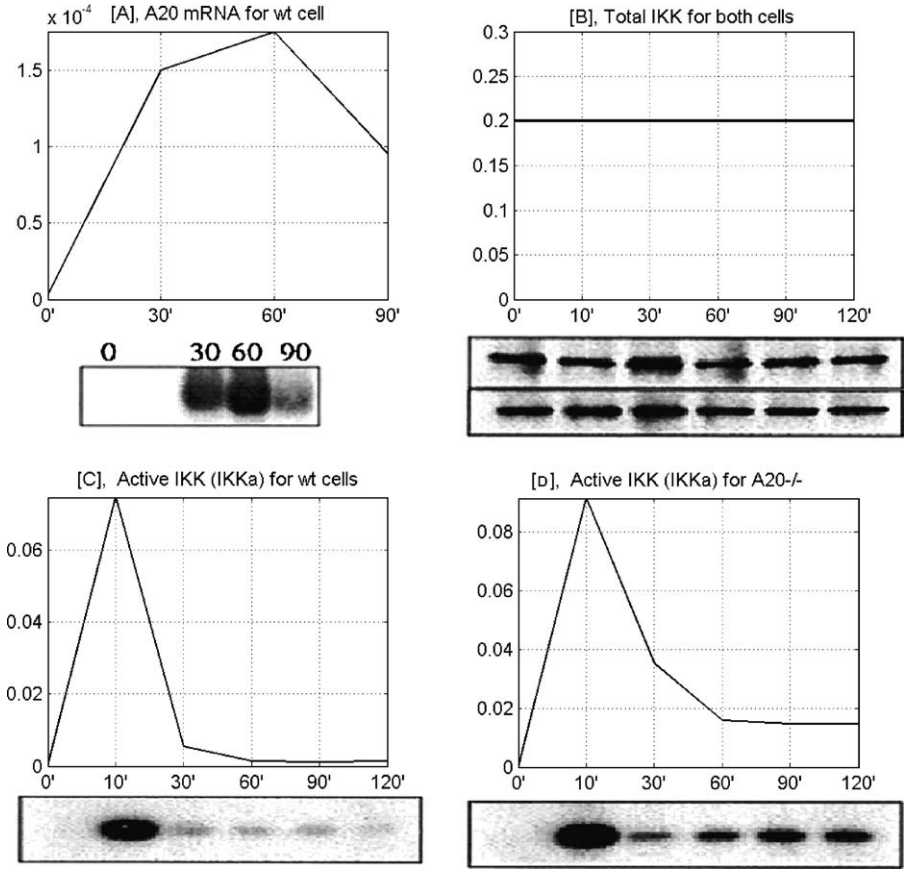

Fig. 6. Model predictions versus measurements by Lee et al. (2000) on wild-type cells and A20 deficient cells with persistent TNF stimulation. The time coordinate is rescaled, and the values of corresponding functions are calculated based on the fitted parameters, at the same time points as in the experiment. The concentrations are given in μM. (A) A20 mRNA for wild-type cells. (B) Model-predicted total $IKK = IKKn + IKKa + IKKi$ versus experiment, wild type in upper panel, and A20−/− in lower panel. According to the model total IKK remains constant. (C and D) Model-predicted IKKa versus IKK kinase activity, respectively for wild-type and A20−/− cells.

amplified in the rest of the system response. In Figs. 7A and B we compare the profiles of IκBα protein for wild-type and $A20^{-/-}$ cells. In both types of cells, the TNF signal causes an equally sharp decrease in the IκBα level, but in wild-type cells, the IκBα rebounds 60 min after the start of the TNF treatment. The fact that IκBα is not detectable in $A20^{-/-}$ cells is caused by the prolonged IKK activity, which is sufficiently high to degrade much of the newly synthesized protein. This is in general agreement with our model, which predicts that IκBα in $A20^{-/-}$ cells remains at a relatively low, possibly undetectable level. For wild-type cells, our model produces a second minimum after 2 h, which agrees with the measurements of Hoffmann et al. (2000), but not with those of Lee et al. (2000) where after 2 h the IκBα level is still high. However, such differences can be due to different cell culture used in both experiments. In Fig. 7D, we observe that the IKK in $A20^{-/-}$ cells dysregulates NF-κB activity; once NF-κB accumulates in the nucleus it remains there throughout the TNF stimulation. In the wild-type cells, NF-κB also accumulates in the nucleus 30 min after the start of TNF treatment, but the newly synthesized IκBα binds to it and leads it into cytoplasm, Fig. 7C. For both types of cells the maximum concentration of NF-κB, after 30 min, assayed by EMSA, appears to be comparable. This suggests that almost all the protein is then in the nucleus, which agrees with our predictions. The prolonged NF-κB activation in $A20^{-/-}$ cells leads to two-fold higher IκBα mRNA abundance at the end of TNF stimulation (Fig. 7F) compared to that observed in wild-type cells (Fig. 7E). Note that in our case, the high level of mRNA transcript coincides with the low protein level, which is much smaller in A20-deficient cells than in wild-type cells.

3.3. Analysis of the regulatory mechanisms in the system

The NF-κB regulatory system we proposed involves two activators, IKK and NF-κB, and two inhibitors, A20 and IκBα. We now analyse how the system behaves at various inhibitor and activator levels.

In Fig. 8, we show the dynamics of total cytoplasmic IκBα, free NF-κB and cgen mRNA level during

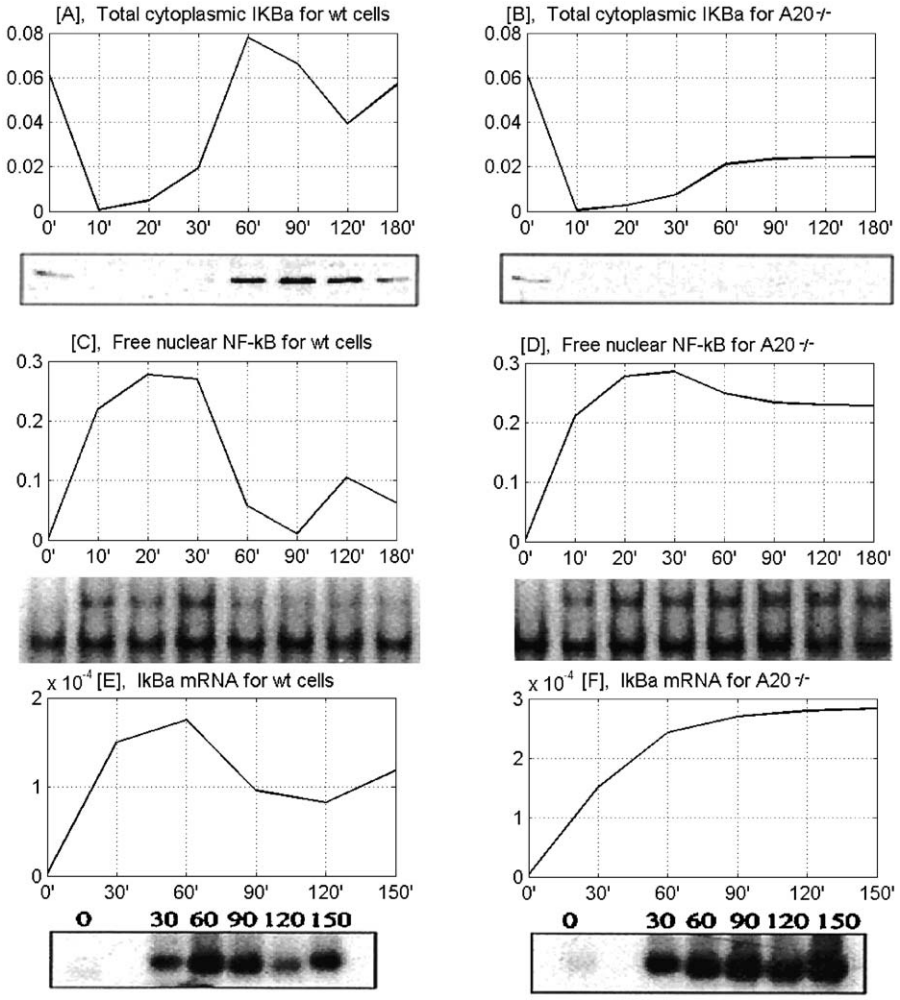

Fig. 7. Model predictions versus Lee et al. (2000) measurements, continued from Fig. 6. (A and B) total cytoplasmic IκBα, respectively for wild-type cells and A20−/− cells. (C and D) NF-κB assayed by EMSA, respectively, for wild-type cells and A20−/− cells. (E and F) mRNA IκBα transcript, respectively, for wild-type cells and A20−/− cells. Note the inverse correspondence between transcript and protein levels, panels A and E, and B and F.

persistent TNF stimulation. First, calculated for the best fit parameters (reference case, see Tables 1–4 in the Appendix), then with A20 or IκBα mRNA transcription coefficients c_1 or c_{1a} elevated three-fold with respect to the best fit value (the other coefficients are unchanged). The higher level of A20 mRNA transcript leads to a higher level of A20 protein (not shown). Since A20 inactivates IKK, higher level of A20 lowers the peak of IKKa and, even more importantly its tail (not shown). The effect of lower IKK activity is that it takes longer to degrade IκBα, and as a result the oscillation period is longer (compare Fig. 7E with B). The oscillations are much less damped, but still the system under an extended TNF activation reaches the steady state characterized by a lower level of free NF-κB (0.053 versus 0.084 μM in reference case) and proportionately lower level of cgen mRNA concentration (6.7×10^{-5} versus 1.05×10^{-4} μM). It is interesting to observe that although the asymptotic level of mRNA IκBα is now substantially lower (6.7×10^{-5}, versus 1.05×10^{-4} μM in reference case), the asymptotic level of the total IκBα cytoplasmic protein is slightly higher (0.0555 versus 0.051 μM), which is due to a lower IKK activity. Again, we observe the inverse correspondence between IκBα message and protein. For even larger c_1, the stability of the steady state is lost and for $3.5 \times 10^{-4} \gtrsim c_1 \gtrsim 2.5 \times 10^{-6}$, the system under extended TNF activation reaches a periodic orbit. Only for unrealistically large $c_1 \gtrsim 3.5 \times 10^{-4}$ the oscillations are again damped and the system reaches a steady state.

After changing the IκBα mRNA coefficient c_{1a} to a level three times higher than the reference level (Figs. 8G–I), the oscillations are less damped than in the reference case, but the system still converges to a steady state. A higher level of IκBα mRNA leads in this case to a higher IκBα protein level, and consequently to a lower asymptotic level of free NF-κB (asymptotic value 0.049 μM) and mRNA of A20 and of the cgen

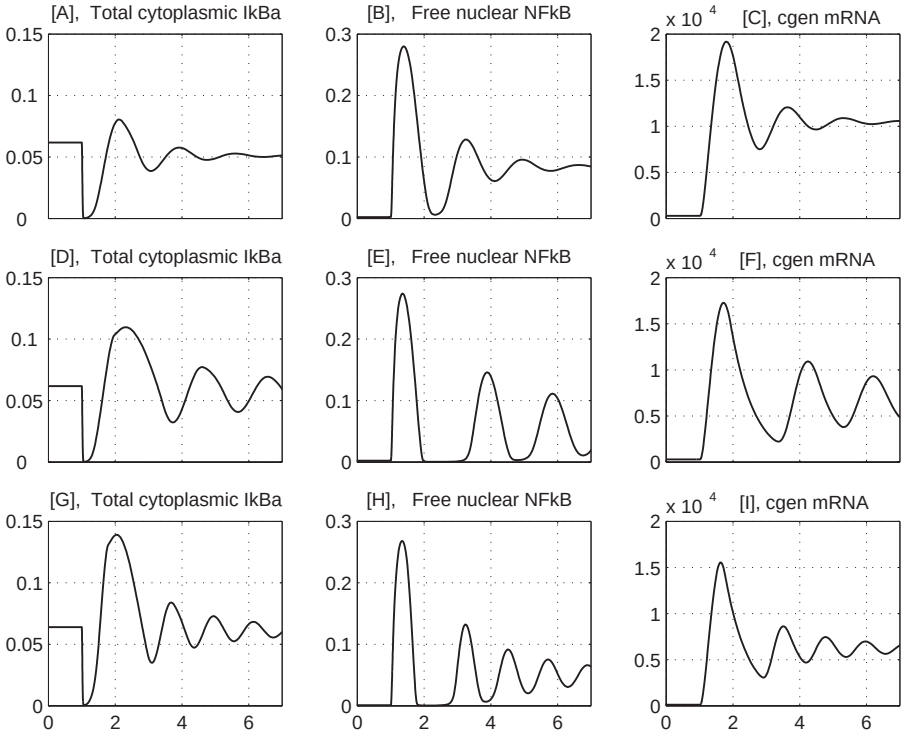

Fig. 8. Dynamics of total cytoplasmic IκBα, free NF-κB and cgen mRNA level during persistent TNF stimulation (started at 1 h). In panels A–C, the fitted parameters were used. In panels D–F, A20 mRNA transcription coefficient c_1 was elevated three-fold with respect to the best fit value. In panels G–I, IκBα mRNA transcription coefficient c_{1a} was elevated three-fold with respect to the best fit value. The concentrations are given in μM, time is in hours.

(6.2×10^{-5} μM). For even larger c_{1a}, the stability of the steady point is lost and for c_{1a} in the relatively narrow range $8 \times 10^{-6} \gtrsim c_{1a} \gtrsim 5 \times 10^{-6}$, the system has a stable periodic orbit. Let us note that a three-fold elevation of the mRNA synthesis coefficient of any two inhibitors causes a comparable decrease in the level of cgen: to 6.7×10^{-5} μM in the case when the production term of mRNA IκBα is elevated and to 6.2×10^{-5} μM when production of A20 is elevated.

In Fig. 9, we analyse the system response caused by the change of IKK or NF-κB levels, the reference case is shown in Figs. 8A–C. A three-fold increase in IKK production rate (Figs. 9A–C) causes strong damping of the oscillations and, as expected, an increase in average levels of free NF-κB (asymptotic value 0.127 μM) and mRNA levels of IκBα, A20 and cgen, the asymptotic value of which is now $cgen_t = 1.59 \times 10^{-4}$ μM. Lowering the IKK production rate causes an effect similar to that of increasing the A20 transcription rate, and correspondingly, the effect caused by increasing IKK production rate resembles the effect caused by lowering the A20 transcription rate. These findings indicate a tight regulation between IKK and its inhibitor A20. Interestingly, the three-fold increase of transcription coefficients of IκBα, A20 or of the IKK production rate causes relatively smaller deviation (less than 50%) in the level of cgen, which indicates good regulatory properties of the considered module.

Since NF-κB is the principal activator in the module, we consider both its three-fold increase (Figs. 9–F) and threeold decrease (Figs. 9G–I). Since the total amount of NF-κB is assumed to be constant it is adjusted by changing the initial condition, i.e. the value of the coefficient N_F. An increase in total NF-κB makes the oscillations less dampened but the system, under persistent activation, still converges to a stable state. The average level of free NF-κB is higher (with asymptotic value 0.161 μM), which implies higher average levels of mRNA of IκBα, A20 and of the cgen, (the asymptotic value of which is 2.02×10^{-4} μM) but strong oscillations in their levels are present. A three-fold increase of NF-κB has a much stronger effect on the rest of the regulatory module than the same change of IKK or of the two inhibitors. Interestingly, an increase of NF-κB triggers the oscillations, while the increase of the second activator IKK shuts them down. It is necessary to be very cautious in making such predictions since it is quite possible that in reality such large increase in NF-κB nuclear level will cause a much smaller increase of mRNA transcription speed, which, even for the endogenous NF-κB level, is close to the physiological maximum (see appendix). The NF-κB decrease also has significant consequences. It smoothes out the oscillations and causes the asymptotic levels of mRNA of IκBα, A20 and of the cgen (5.0×10^{-5} μM) to become almost twice lower than in the reference case.

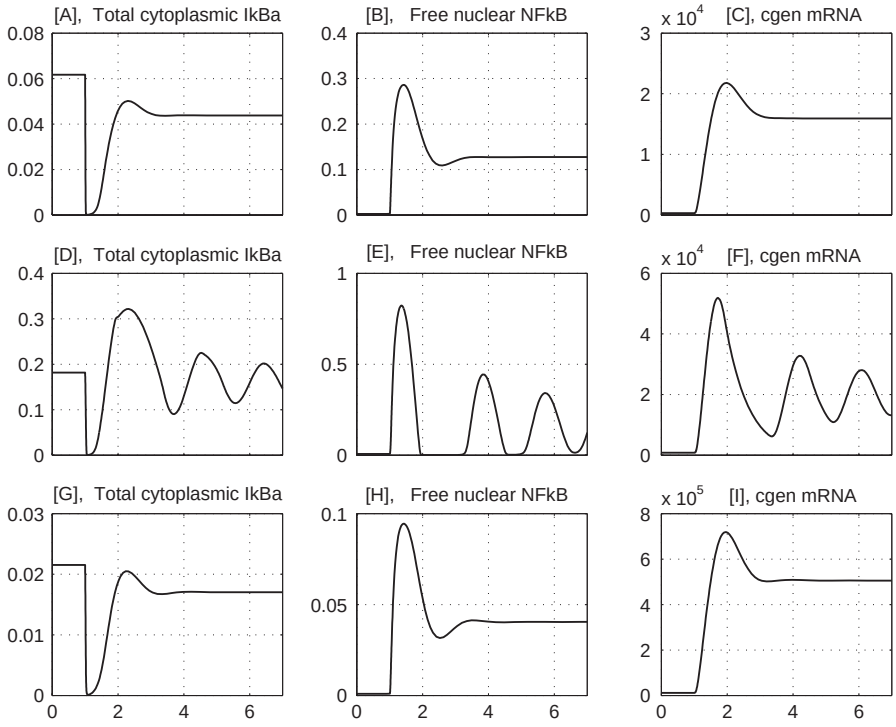

Fig. 9. Dynamics of main variables during persistent TNF stimulation (started at 1 h). In panels A–C, the IKKn production rate k_{prod} was elevated three-fold with respect to the best fit value. In panels D–F, the total NF-κB amount was elevated three-fold with respect to the best fit value. In panels G–I, the total NF-κB amount was lowered three-fold with respect to the best fit value. All plots should be compared with Fig. 8A, in which the best fit parameters were used.

4. Model limitations

The proposed model involves a very restricted number of components: RNA transcripts, proteins and complexes, which were found to be the most important ones. Using this limited number of components we attempted to model the NF-κB regulatory module, which in fact involves a much larger set of components, and whose true kinetics is much more complicated. There are two main reasons for the simplifications we made. First, we do not have enough data, second a more elaborate model would be possibly too difficult to analyse; at least the parameter fitting would be both very difficult and ambiguous. Let us point out the main simplifications and implicit assumptions of the model:

1. The two model components: NF-κB or IKK are protein complexes themselves, and the complicated kinetics leading to their formation is neglected. The predominant form of NF-κB is a heterodimer composed of RelA (p65) and NF-κB1 (p50). While RelA is synthesized as a mature product, the second component is synthesized as a large precursor p105, containing an N-terminal Rel homology domain, and C-terminal ankyrin repeat domain, homologous with IκB proteins. Then, a C-terminal of p105 is cleaved out to produce p50. This proteolytic processing is possibly signal dependent (via phosphorylation on C-terminus; MacKichan et al., 1996) and requires polyubiquitination. Moreover, the synthesis of p105 is NF-κB dependent. Fortunately, the synthesis of RelA, the crucial NF-κB component, appears to be signal independent and constant. This is why we expect that the production of NF-κB heterodimers is constant and may be balanced by degradation, and we assume that total amount of NF-κB remains constant. Similarly, the unresolved kinetics leading to formation of IKK tetrameric complexes is approximated in our model by de novo synthesis with a constant production term.
2. The inhibitory proteins A20 and IκBα mimic a collective action of groups of inhibitors. IκBα represents a collective action of whole IκB family, but also for p105 and p100, whose C-terminus, homologous to IκB, may account for their inhibitory action. Similarly, although it was found recently (Heyninck et al., 2003) that the A20-binding inhibitors of NF-κB activation (ABINs) may act independently of A20, and that overexpression of ABIN-1 or ABIN-2 mimics the NF-κB inhibiting effect of A20, our model accounts only for A20. Besides, the model only accounts for the A20 inhibitory action which is on the level of IKK deactivation, while the interaction of A20 with

TNF receptor-associating factors TRAF1 and TRAF2 (Song et al., 1996) is not explicitly taken into account.

3. The implicit assumption we made in our modeling is that all other proteins, some known, some unknown, which we do not account for in the pathway, remain at their normal levels. There are several proteins, like Caspase-8, GSK-3, FADD, FLIP, MEKK3, T2K, involved in TNF-NF-κB signaling, the knockout of which leads to the embryonic lethality (Wajant et al., 2003 and references therein). However, despite the fact that their existence is needed for the functioning of the considered autoregulatory module, we do not take them explicitly into account assuming that they are not involved in any feedback loops with NF-κB, and restricting the model predictions to the case when they remain at their normal levels. Similarly, we do not take into account any possible feedback loop involving the NF-κB dependent genes other than A20 and IκBα. Since NF-κB regulates expression of hundreds of various genes, these additional feedback loops are likely to be discovered.
4. There is a large number of the so-called late genes, which are NF-κB regulated and which contain κB sites in their promotory regions, but whose transcripts start to accumulate several hours after the NF-κB entering the nucleus. Possibly the additional factors are needed to stimulate their transcription, but the problem is not resolved yet. Our model may not produce any predictions for the kinetics of these late genes.
5. A number of recent studies support the conjecture that RelA phosphorylation may be necessary for transcriptional competence of NF-κB (Ghosh and Karin, 2002, and references therein). In the model, we simply assume that the NF-κB is in a state in which it is capable of regulating transcription. The two recent experiments of Yamamoto et al. (2003) and Anest et al. (2003) indicated that IKKα is a possible nuclear coactivator of the IκBα and IL-8 promoters. Both groups have found that IKKα interacts with the CREB-binding protein and in conjunction with RelA it is requited to NF-κB responsive promoters and mediates the cytokine-induced phosphorylation and subsequent acetylation of specific residues in histone H3, which is critical for NF-κB-induced gene expression.

5. Discussion

The present paper is the second to analyse the complex NF-κB regulatory module by means of a relatively simple mathematical model, which takes into account a limited number of proteins and their complexes. The first attempt was made by Hoffmann et al. (2002) who concentrated on the interplay between IκB isoforms: IκBα, IκBβ, and IκBε. In our work, we approximated the collective action of all IκB isoforms by the IκBα, which is the most active and abundant one, and the knockout of which, in contrast to the other two isoforms, is lethal (Gerondakis et al., 1999, and references therein). After this simplification we concentrated on two new issues:

(1) The two-compartment dynamics of IκBα, NF-κB and the (IκBα|NF-κB) complexes. Hoffmann et al. (2002) have considered transport between nucleus and cytoplasm, but they assumed that the sum of cytoplasmic and nuclear concentrations of diffusing substrates remains constant, which can be only justified when the cytoplasmic and nuclear volumes are equal. In most cases, however, the cytoplasm is substantially larger than the nucleus.
(2) The main issue we focused on was the kinetics of the activator IKK and its inhibitory protein A20. The importance of its inhibitory potential was demonstrated by Lee et al. (2000), who found that the knockout of A20 in mice dramatically alters the cells response to TNF stimulation due to persistent IKK activity, and causes A20$^{-/-}$ deficient mice to die prematurely.

We have reconsidered also the resting cell steady state, by taking into account experimental constraint on the level of free IκBα; according to Rice and Ernst (1993) excess of IκBα is less than 15% relative to NF-κB.

The considerations on the two-compartment dynamics showed that the ratio of cytoplasmic to nuclear volume, k_v, is an additional important parameter, which regulates the kinetics of the entire network. In all previous considerations we assumed $k_v = 5$, but obviously different cells may have considerably different values of k_v. In the case of fibroblasts, the ratio of nuclear to cytoplasmic volume depends also on the cell activity or the stage of the cell cycle. Mature cells usually have larger k_v than young, active cells, in which the nucleus occupies the larger part of the cell. This implies, not only the existence of different kinetics for different cell types, but also that the cellular response may depend on its stage in cell cycle. To see how the cell response depends on the value of k_v, let us fix all other parameters on the previous level, and simulate the model equations first for $k_v = 2$ (Figs. 10D–F) then for $k_v = 10$ (Figs. 10G–I). Keeping all other parameters on the same level implies that we are changing k_v by change of the nuclear rather than cytoplasmic volume, since perturbation of cytoplasmic volume influences several other parameters. For $k_v = 2$, we observe much stronger oscillation damping than in the reference case. The whole kinetics resembles the one presented in Figs. 9G–I, where the total amount of NF-κB was three-fold lowered compared to the reference case. This

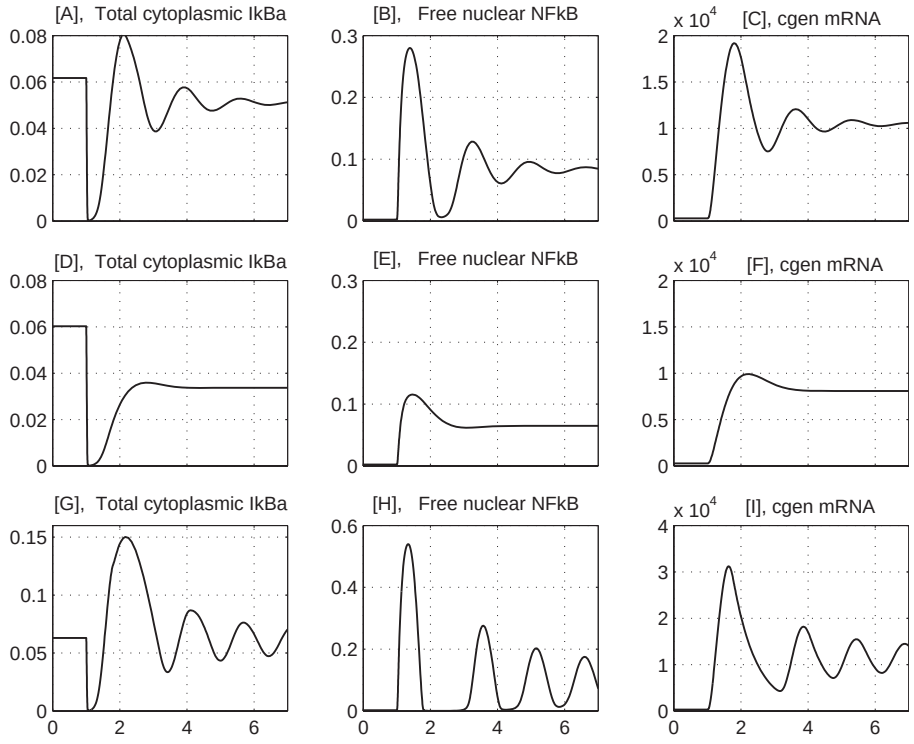

Fig. 10. Dynamics of main variables during persistent TNF stimulation (started at 1 h). In panels A–C, the ratio of cytoplasmic to nuclear volume is $k_v = 5$, as in rest of the paper. In panels D–F, the ratio of cytoplasmic to nuclear volume has been lowered to $k_v = 2$. In panels G–I, the ratio of cytoplasmic to nuclear volume has been elevated to $k_v = 10$.

is due to the fact that a relatively larger nucleus implies a smaller NF-κB concentration, which, as already found, implies smaller oscillations and lower asymptotic levels of NF-κB dependent genes. Conversely, a smaller nucleus implies that NF-κB nuclear concentration is higher, which causes larger oscillations, and higher levels of NF-κB dependent transcripts and proteins, Figs. 10G–I. The kinetics $k_v = 10$ resembles that in Figs. 9D–F where a three-fold higher level of total NF-κB was assumed. The above analysis shows that a change of nuclear volume, with other parameters unchanged, considerably alters kinetics of the NF-κB module. The change of the cytoplasmic volume also substantially alters cell response since it influences both k_v and all V-dependent coefficients of transcription and transport. However, since it seems reasonable that alternation of nuclear or cytoplasmic volumes results in some adaptation of other parameters, a more detailed analysis is needed to account for the possible effects caused by that alternation.

Inclusion of A20 revealed the second important feedback loop in the NF-κB regulatory network. Like IκBα, the A20 is a NF-κB inducible protein, which acts as a NF-κB inhibitor. The knockout of either of these two genes leads to prolonged NF-κB activity, which, once enters the nucleus is not effectively shuttled out of it (Lee et al., 2000, Fig. 3A, Hoffmann et al., 2002, Figs. 2A and 4C). However, the inhibitory actions of these two proteins are different. The newly synthesized IκBα inhibits NF-κB in a direct way, entering the nucleus and shuttling NF-κB back into a sequestered state in the cytoplasm. The action of A20 is indirect: it promotes transformation of the active IKKa to IKKi, a form, which is no longer capable of phosphorylating IκBα. As a result of inactivating IKK, A20 rescues IκBα, allows that it accumulates in cytoplasm, and thus enables its inhibitory action. In A20-deficient cells, IκBα is continuously and almost completely degraded by IKK and cannot terminate the NF-κB residence. This is why the knockout of any of these two genes leads to similar downstream consequences.

Acknowledgements

The MATLAB program written to perform the calculations will be available at the website: http://www.stat.rice.edu/~mathbio/NF-kappaBmodel. This work was supported by NHLBI contract N01-HV-28184, Proteomic technologies in airway inflammation (A. Kurosky, P.I.). One of the authors, Tomasz Lipniacki, was supported, in part, by KBN Grant No. 8T07A 045 20.

Appendix. Model parameters

The coefficient a_1 (see Table 1) was adopted from Hoffmann et al. (2002), who deduced it based on the works of Carlotti et al. (2000) and Malek et al. (1998). The coefficients a_2 and t_1 assumed here are much larger than those in Hoffmann et al. (2002) ($a_2 = 0.0225$, $a_3 = 0.185$), which were based on works of Heilker et al. (1999) and Zandi et al. (1998). In the above experiments, the authors measured the average catalytic activity of the whole IKK, while in our model we consider the three states of IKK. Only one of them is active, so that one may expect that its activity, which is regulated by coefficients a_2 and t_1, is significantly higher. The measurements in Lee et al. (2000, Fig. 3E) show a narrow, very tall peak in IKK activity, followed by a lower tail. In wild-type cells it appears that the IKK activity decreases much more than 10 times, while in A20-deficient cells it decreases about five times. However, it remains on the level high enough to degrade much of the IκBα and, as a consequence, most of NF-κB remains in the nucleus. In our model, the activity of all IKK is proportionate to the amount of IKKa, the active form, hence we may deduce that one-tenth of the maximal concentration leads to saturation in NF-κB, which implies a very high activity of the active part of IKK. If we adopted the same parameter values for IKKa as Hoffmann did for total IKK, we would need unrealistically high total IKK concentrations. The works of Heilker et al. (1999) and Zandi et al. (1998) prove that the catalysis of IKK complexes proceeds very fast. Based on these works, Hoffmann et al. (2002) assumed $t_1 = 0.037$ and $t_2 = 0.185$. One can expect again that, for the active portion of IKK, these coefficients are higher. We assume for calculations $t_1 = t_2 = 0.1$, after checking that any larger value will give almost the same results. Making coefficients t_1 and t_2 even larger does not make the IκBα degradation proceed faster, because for large t_1 and t_2 coefficients the efficiency of the process is limited by the formation of complexes, not by their catalysis.

The average volume of a fibroblast cell is $V + U = 2000\ \mu m^3 = 2 \times 10^{-12}\ l$ (Carlotti et al., 1999), and we adopt this value for further estimations. We will also assume that the ratio of cytoplasmic and nuclear volumes is $k_v = V/U = 5$. Therefore, the cytoplasmic concentration of 1 μM corresponds to $N = 10^{-6}\ (\mathrm{mol/l}) \times V \times Av \approx 10^6$ molecules, where

Table 1
Two- and three-component interactions between IκBα, NF-κB and IKKa

Symbol	Values	Units	Description	Comments
a_1	0.5	$\mu M^{-1}\ s^{-1}$	IκBα−NFκB association	Hoffmann et al. (2002)
a_2	0.2	$\mu M^{-1}\ s^{-1}$	IKKa–IκBα association	Assumption
t_1	0.1	s^{-1}	IKKa|IκBα catalysis	Any large
a_3	1	$\mu M^{-1}\ s^{-1}$	IKKa-(IκBα|NF-κB) association	Assumption
t_2	0.1	s^{-1}	(IKK|IκBα|NF-κB) catalysis	Any large

Table 2
A20 and IκBα synthesis and degradation, IKK dynamics and total amount of free and complexed NF-κB

Symbol	Values	Units	Description	Comments
c_{1a}	5×10^{-7}	s^{-1}	IκBα-inducible mRNA synthesis	Assumption
c_{2a}	0.0	$\mu M\ s^{-1}$	IκBα-constitutive mRNA synthesis	Assumption
c_{3a}	0.0004	s^{-1}	IκBα mRNA degradation	Fitted, Blattner et al.
c_{4a}	0.5	s^{-1}	IκBα translation rate	Fitted
c_{5a}	0.0001	s^{-1}	Spontaneous, free IκBα protein degradation	Pando and Verma (2000)
c_{6a}	0.00002	s^{-1}	IκBα degradation (complexed to NF-κB)	Pando and Verma (2000)
c_1	5×10^{-7}	s^{-1}	A20-inducible mRNA synthesis	Assumption
c_2	0.0	$\mu M\ s^{-1}$	A20-constitutive mRNA synthesis	Assumption
c_3	0.0004	s^{-1}	A20 mRNA degradation	Assumption
c_4	0.5	s^{-1}	A20 translation rate	Assumption
c_5	0.0003	s^{-1}	A20 protein degradation	Fitted
k_1	0.0025	s^{-1}	IKK activation rate caused by TNF	Fitted
k_2	0.1	s^{-1}	IKK inactivation rate caused by A20	Fitted
k_3	0.0015	s^{-1}	IKK spontaneous inactivation rate	Fitted
k_{prod}	0.000025	$\mu M\ s^{-1}$	IKKn production rate	Fitted
k_{deg}	0.000125	s^{-1}	IKKa, IKKn and IKKi degradation	Fitted
N_F	$0.06\ V$	μM V	Total amount of free and complexed NF-κB	Assumption, Carlotti

Table 3
Transport between compartments, and assumed $k_v = V/U$, ratio of cytoplasmic and nuclear volumes

Symbol	Value	Units	Description	Comments
$k_v = V/U$	5		Cytoplasmic to nuclear volume	Assumption
i_1	0.0025	s^{-1}	NF-κB nuclear import	Fitted
e_{2a}	0.01	s^{-1}	(IκBα|NF-κB) nuclear export	Fitted
i_{1a}	0.001	s^{-1}	IκBα nuclear import	Fitted
e_{1a}	0.0005	s^{-1}	IκBα nuclear export	Assumption

Table 4
Assumed *cgen* parameters

Symbol	Value	Units	Description	Comments
c_{1c}	5×10^{-7}	s^{-1}	cgen inducible mRNA synthesis	Assumption
c_{2c}	0.0	$\mu M\ s^{-1}$	cgen constitutive mRNA synthesis	Assumption
c_{3c}	0.0004	s^{-1}	cgen mRNA degradation	Assumption

$Av = 6.022 \times 10^{23}$ molecules/mol is the Avogadro number. Respectively, the same nuclear concentration corresponds to 2×10^5 molecules. The total amount of NF-κB is kept constant in the course of simulation, and it is set by assuming the initial concentration of cytoplasmic complexes (IκBα|NF-κB). The assumed amount of total NF-κB (see Table 2) corresponds to the average cellular concentration $cc = 0.06\ \mu M\ V/(V+U) = 0.05\ \mu M$, which agrees with Carlotti et al. (1999) who, based on transfection experiments with EGFPRelA, estimated that the endogenous level of RelA expression is $\sim 60,000$ molecules per cell, and then Carlotti et al. (2000) concluded that overall cell concentration is 0.05 μM. The efficiency of the transcriptional machinery gives the upper bound on the mRNA synthesis coefficients c_1, c_2 and c_{1a}, c_{2a}. The typical transcription speed in animal cells is of the order of 40 nucleotides (nt) per second (Levin, 2000, p. 129). A single gene, however, can be read by a number of RNA polymerases simultaneously (see e.g. Levin, p. 128, Fig. 5.13). Assuming that the smallest possible spacing between subsequent RNA polymerases is of order 250 nt (the single polymerase covers about 20–30 nt of the DNA strand), one obtains the transcription initiation frequency $\nu = 40/250 = 0.16/s$. Therefore, we assume that maximum mRNA production rate is 0.16 mRNA/s or 1.6×10^{-7} μM/s, when mRNA concentration is counted per cytoplasmic volume V. We assume also that this rate may be attained when all NF-κB is present in the nucleus, which implies that its nuclear concentration is 0.3 μM. As a result we obtain the IκBα mRNA inducible synthesis coefficient as equal to $c_{1a} = (1.6 \times 10^{-7}\ \mu M/s)/0.3\ \mu M \approx 5 \times 10^{-7}/s$. We assumed $c_{2a} = 0$, but any $c_{2a} \leqslant 1.5 \times 10^{-9}$ would be reasonable; $c_{2a} = 1.5 \times 10^{-9}$ implies that in the resting cells about 15% of total IκBα is free, which is the upper bound according to Rice and Ernst (1993). The IκBα translation coefficient $c_{4a} = 0.5/s$ results from the assumed mRNA synthesis coefficient c_{1a}, since the effective protein production rate is proportional to the product of these two coefficients. The value of c_{4a} is well justified (Levin, 2000, pp. 125–126); it corresponds to a translation speed of 15 aminoacids (a.a.) per second, in each of the 10 ribosomes simultaneously processing a single mRNA transcript of length of 900 nt, which leads to a 300 a.a. protein (mouse IκBα is 314 a.a. long, while human IκBα is 317 a.a. long). It results from our fitting, that both synthesis and translation of IκBα proceed at the highest possible speed. The coefficient of IκBα mRNA degradation $c_{3a} = 0.0004$ (which corresponds to $t_{1/2} \approx 30$ min) was fitted, but it is in accordance with Blattner et al. (2000) measurements, who found that spontaneous half-life of IκBα mRNA is within the range from 15 to 30 min. As already said, we have significant freedom in choosing some parameters, and this is why we decided to assume that the mRNA synthesis, degradation and translation rates are equal for A20 and IκBα. The protein degradation rate, however, was then found to be three times larger for A20 than for IκBα. This is caused by the fact that IκBα is degraded both spontaneously and catalytically. The large degradation rate of A20 suggests that it is also possibly degraded in some active way. The assumption that all forms of IKK, i.e. IKKn, IKKa and IKKi degrade with the same degradation rate implies that total amount of IKK remains on a constant level, which is supported by Lee et al. (2000, Fig. 3E) measurements.

We have fitted the transport coefficients (Table 3) to the data from Hoffmann et al. (2002) and Lee et al. (2000) experiments. However, one should remember, that these coefficients scale as $1/V$, or as S/V, if one assumes that transport through nuclear membrane is

proportional to its surface S. Coefficient i_1 of NF-κB nuclear import is much smaller than that used by Hoffmann et al. (2002), who used $i_1 = 0.09$, but here it accounts for the delay caused by IκBα ubiquitination and proteolytic degradation, see Section 2.1. The fitted value implies that the half-life time of phosphorylated IκBα is $\sim$5 min. The value of e_{1a} reflects the assumption that $i_{1a}/e_{1a} \approx 2$, which is supported by Yang et al. (2001, Fig. 1) experiments, see our Section 2.3. The assumed cgen parameters are given in Table 4.

References

Anest, V., Hanson, J.L., Cogswell, P.C., Steinbrecher, K.A., Strahl, B.D., Baldwin, A.S., 2003. A nucleosomal function for IκB kinase-α in NF-κB-dependent gene expression. Nature 423, 659–663.

Arvelo, M.B., Cooper, J.T., Longo, C., Soizic, D., Grey, S.T., Mahiou, J., Czismadia, E., Abu-Jawdeh, G., Ferran, C., 2002. A20 protects mice from D-galactosamine/lipopolysaccharide acute toxic lethal hepatitis. Hepatology 35, 535–543.

Beyaert, R., Heyninck, K., Van Huffel, S., 2000. A20 and A20-binding proteins as cellular inhibitors of nuclear factor-kappa B-dependent gene expression and apoptosis. Biochem. Pharmacol. 60, 1143–1151.

Blattner, C., Kannouche, P., Litfin, M., Bender, K., Rahmsdorf, H.J., Angulo, J.F., Herrlich, P., 2000. UV-induced stabilization of c-fos and other short-lived mRNAs. Mol. Cell. Biol. 20, 3616–3625.

Caamano, J., Hunter, C.A., 2002. NF-κB family of transcription factors: central regulators of innate and adaptive immune functions. Clin. Microbiol. Rev. 15, 414–429.

Carlotti, F., Dower, S.K., Qwarnstrom, E.E., 2000. Dynamic shuttling of nuclear factor kappa B between the nucleus and cytoplasm as a consequence of inhibitor dissociation. J. Biol. Chem. 275, 41028–41034.

Carter, R.S., Geyer, B.C., Xie, M., Acevedo-Suarez, C.A., Ballard, D.W., 2001. Persistent activation of NF-κB by the tax transforming protein involves chronic phosphorylation of IκB kinase subunits IKKβ and IKKγ. J. Biol. Chem. 276, 24445–24448.

Chen, F.E., Huang, D., Chen, Y., Ghosh, G., 1998. Crystal structure of p50/p65 heterodimer of transcription factor NF-κB bound to DNA. Nature 391, 410–413.

Delhase, M., Hayakawa, M., Chen, Y., Karin, M., 1999. Positive and negative regulation of IκB kinase activity through IKKβ subunit phosphorylation. Science 284, 309–313.

Gerondakis, S., Grossmann, M., Nakamura, Y., Pohl, T., Grumont, R., 1999. Genetic approaches in mice to understand Rel/NF-κB and IκB function: transgenics and knockouts. Oncogene 18, 6888–6895.

Ghosh, S., Karin, M., 2002. Missing pieces in the NF-κB puzzle. Cell 109, S81–S96.

Ghosh, S., May, M.J., Kopp, E.B., 1998. NF-κB and Rel Proteins: evolutionary conserved mediators of immune responses. Annu. Rev. Immunol. 16, 225–260.

He, K.-L., Ting, A.T., 2002. A20 Inhibits tumor necrosis factor (TNF) alpha-induced apoptosis by disrupting recruitment of TRADD and RIP to the TNF receptor 1 complex in jurkat T cells. Mol. Cell. Biol. 22, 6034–6045.

Heilker, R., Freuler, F., Vanek, M., Pulfer, R., Kobel, T., Peter, J., Zerwes, H.G., Hofstetter, H., Eder, J., 1999. The kinetics of association and phosphorylation of IκB isoforms by IκB kinase 2 correlate with their cellular regulation in human endothelial cells. Biochemistry 38, 6231–6238.

Heyninck, K., Kreike, M.M., Beyaert, R., 2003. Structure–function analysis of the A20-binding inhibitor of NF-κB activation, ABIN-1. FEBS Lett. 536, 135–140.

Hoffmann, A., Levchenko, A., Scott, M.L., Baltimore, D., 2002. The IκB-NF-κB signaling module: temporal control and selective gene activation. Science 298, 1241–1245.

Karin, M., 1999. The beginning of the end: IκB kinase (IKK) and NF-κB activation. J. Biol. Chem. 274, 27339–27342.

Krikos, A., Laherty, C.D., Dixit, V.M., 1992. Transcriptional activation of the tumor necrosis factor alpha-inducible zinc finger protein, A20, is mediated by kappa B elements. J. Biol. Chem. 267, 17971–17976.

Kunsch, C., Ruben, S.M., Rosen, C.A., 1992. Selection of optimal kappa B/Rel DNA-binding motifs: interaction of both subunits of NF-kappa B with DNA is required for transcriptional activation. Mol. Cell. Biol. 12, 4412–4421.

Lee, E.G., Boone, D.L., Chai, S., Libby, S.L., Chien, M., Lodolce, J.P., Ma, A., 2000. Failure to regulate TNF-induced NF-κB and cell death responses in A20-deficient mice. Science 289, 2350–2354.

Levin, B., 2000. Genes, Vol. VII. Oxford University Press, Oxford.

Li, T., Narhi, L.O., Wen, J., Philo, J.S., Sitney, K., Inoue, J., Yamamoto, T., Arakawa, T., 1998. Interactions between NF-κB and its inhibitor IκB: biophysical characterization of NF-κB IκBα complex. Journal of Protein Chemistry 17 (8), 757–763.

MacKichan, M.L., Logeat, F., Israel, A., 1996. Phosphorylation of p105 PEST sequence via a redox-insensitive pathway upregulates processing of p50 NF-κB. J. Biol. Chem. 271, 6084–6091.

Malek, S., Huxford, T., Ghosh, G., 1998. IκBα functions through direct contacts with the nuclear localization signals and the DNA binding sequences of NF-κB. J. Biol. Chem. 273, 25427–25435.

Pando, M.P., Verma, I.M., 2000. Signal-dependent and -independent degradation of free and NF-κB-bound IκBα. J. Biol. Chem. 275, 21278–21286.

Rice, N.R., Ernst, M.K., 1993. In vivo control of NF-κB activation by IκBα. EMBO 12, 4685–4695.

Rodriguez, M.S., Thompson, J., Hay, R.T., Dargemont, C., 1999. Nuclear retention of IκBα protects it from signal-induced degradation and inhibits nuclear factor κB transcriptional activation. J. Biol. Chem. 274, 9108–9115.

Song, H.Y., Rothe, M., Goeddel, D.V., 1996. The tumor necrosis factor-inducible zinc finger protein A20 interacts with TRAF1/TRAF2 and inhibits NF-κB activation. Proc. Natl Acad. Sci. USA 93, 6721–6725.

Sun, S.-C., Ganchi, P.A., Ballard, D.W., Greene, W.C., 1993. NF-κB Controls expression of inhibitor IκBα: evidence for an inducible autoregulatory pathway. Science 259, 1912–1915.

Tangethoff, S., Behlke, J., Scheidereit, C., 2003. Tetrameric oligomerization of IκB kinase γ (IKKγ) is obligatory for IKK complex activity and NF-κB activation. Mol. Cell. Biol. 23, 2029–2041.

Tian, B., Brasier, A.R., 2003. Identification of a nuclear factor kappa B-dependent gene network. Recent Prog. Horm. Res. 58, 95–130.

Tian, B., Zhang, Y., Luxon, B.A., Garofalo, P.G., Casola, A., Sinha, M., Brasier, A.R., 2002. Identification of NF-κB-dependent gene networks in respiratory syncytial virus-infected cells. J. Virol. 76, 6800–6814.

Tyson, J.J., Chen, K.C., Novak, B., 2003. Sniffers, buzzers, toggles and blinkers: dynamics of regulatory and signaling pathway in the cell. Curr. Opin. Cell Biol. 15, 221–231.

Wajant, H., Pfiizenmaier, K., Scheurich, P., 2003. Tumor necrosis factor signaling. Cell Death Differ. 10, 45–65.

Yamamoto, Y., Verma, U.N., Prajapati, S., Kwak, Y., Gaynor, R.B., 2003. Histone H3 phosphorylation by IKKα is critical for cytokine-induced gene expression. Nature 423, 655–659.

Yamaoka, S., Courtois, G., Bessia, C., Whiteside, S.T., Weil, R., Agou, F., Kirk, H.E., Kay, R.J., Israël, A., 1998. Complementation

cloning of NEMO, a component of the IκB kinase complex essential for NF-κB activation. Cell 93, 1231–1240.

Yang, L., Chen, H., Qwarnstrom, E.E., 2001. Degradation of IκBα is limited by a phosphorylation/ubiquitination event. Biochem. Biophys. Res. Commun. 285, 603–608.

Yang, L., Ross, K., Qwarnstrom, E.E., 2003. RelA control of IκBα phosphorylation. J. Biol. Chem. 278, 30881–30888.

Zandi, E., Chen, Y., Karin, M., 1998. Direct phosphorylation of IκB by IKKα and IKKβ: discrimination between free and NF-κB-bound substrate. Science 281, 1360–1363.

Zhang, S.Q., Kovalenko, A., Cantarella, G., Wallach, D., 2000. Recruitment of the IKK Signalosome to the p55 TNF receptor: RIP and A20 bind to Nemo (IKKγ) upon receptor stimulation. Immunity 12, 301–311.